AN ABSTRACT OF THE THESIS OF

Hamid Reza Vejdani Noghreiyan for the degree of Master of Science in Mechanical Engineering presented on May 2, 2013.

Title: Control of Spring-Mass Running Robots

Abstract approved: _____

Jonathan W. Hurst

We seek the control strategies that are applicable on legged robots and control them to run in real world as robust and efficient as animals. To achieve this goal, we need to understand the principles of legged locomotion and the control policies that animals use during running. In this study we tried to understand these principles by investigating birds' running experiments, and hypothesized their possible control policies that are important for real machines. We proposed two types of flight phase control techniques inspired from ground running birds for spring-mass running robots and derived mathematical formulas for the optimum design of the passive elements in these robots. For the control policies, we focused on flight phase because adjusting the leg parameters during the flight is very energy efficient and also the overall behavior of the system is very sensitive to the landing conditions that are determined during the flight phase of running. We first considered the change of the leg angle as the only control parameter during the flight phase. In the proposed control policies, three objective functions i) leg peak

force, ii) axial impulse and iii) leg actuator work, all from passive stance phase, were considered to be regulated during running. It turned out that with a simple swing leg policy (constant leg angular acceleration), all the three objective functions can be nearly regulated at the same time, meaning that both goals of damage avoidance and energy efficiency can be fulfilled at once. After that, we investigated the effect of the leg length in addition to the leg angle on the dynamics of the spring-mass running robots. This control policy retains the steady state running by providing the equilibrium gait for each stride. The leg length and leg angle together make it possible for the robot to retain the steady state in the presence of a disturbance while limit the increase of the leg force which if increases may break the leg. In all of the control policies, the robot is purely passive during the stance phase and therefore the dynamics of the system comes from the passive dynamics of the system. Finally, we investigated the effect of the passive dynamics elements on the initiation of running. We derived mathematical formulas that determine the required stiffness and damping for the actuator to achieve the maximum possible performance given the physical limitations of the system.

Control of Spring-Mass Running Robots

by

Hamid Reza Vejdani Noghreiyan

A THESIS

submitted to

Oregon State University

in partial fulfillment of
the requirements for the
degree of

Master of Science

Presented May 2, 2013
Commencement June 2013

Master of Science thesis of Hamid Reza Vejdani Noghreiyan presented on May 2, 2013.

APPROVED:

Major Professor, representing Mechanical Engineering

Head of the School of Mechanical Industrial and Manufacturing Engineering

---

Dean of the Graduate School

I understand that my thesis will become part of the permanent collection of Oregon State University libraries. My signature below authorizes release of my thesis to any reader upon request.

Hamid Reza Vejdani Noghreiyan , Author

ACKNOWLEDGMENTS

I would like to especially thank my major adviser, Jonathan W. Hurst, for all of his guidance and support. I would also like to thank my thesis committee and the professors at Oregon State University whom I had the chance to be in their classes, and many professors at my previous school, Ferdowsi University of Mashhad. As always, I am profoundly thankful towards my family for everything they have been providing for me that I can not even count.

Funding for this work was provided by the Human Frontier Science Program (HFSP) and the National Science Foundation (NSF).

TABLE OF CONTENTS

TABLE OF CONTENTS (Continued)

LIST OF FIGURES

LIST OF FIGURES (Continued)

LIST OF FIGURES (Continued)

LIST OF TABLES

Chapter 1 – Introduction

Despite of the recent remarkable advances in the field of legged robotics, animals can still outperform the legged robots in performance, efficiency and robustness during running in natural environment. Part of this superiority is due to the difference in the actuator mechanisms that robots and animals have, and part of it is due to the superior control policies that animals use during running. In this work we seek to first understand the control principles of running through investigating the animals' behavior and second to propose design formulas for the passive elements of robots' actuators to achieve the best performance for initiating running.

Observations on animals running revealed that the brain is not very engaged in the process of running. Studies on paralyzed animals showed that, even though the brain signals did not engage in running, they still can accomplish this task. Therefore, it seems that what animals do for their running, may be some types of feed-forward control strategy synchronized with a very well-designed passive actuator mechanism.

We begin with spring-loaded inverted pendulum (SLIP) model as the passive dynamics model for running. SLIP is a simple and yet accurate mathematical model for animals and humans running [1]. Recent studies showed that this model has a self-stabilizing characteristic [2], which implies that it does not require control effort to become stable, and hence is aligned with the observations from paralyzed animals stable running.

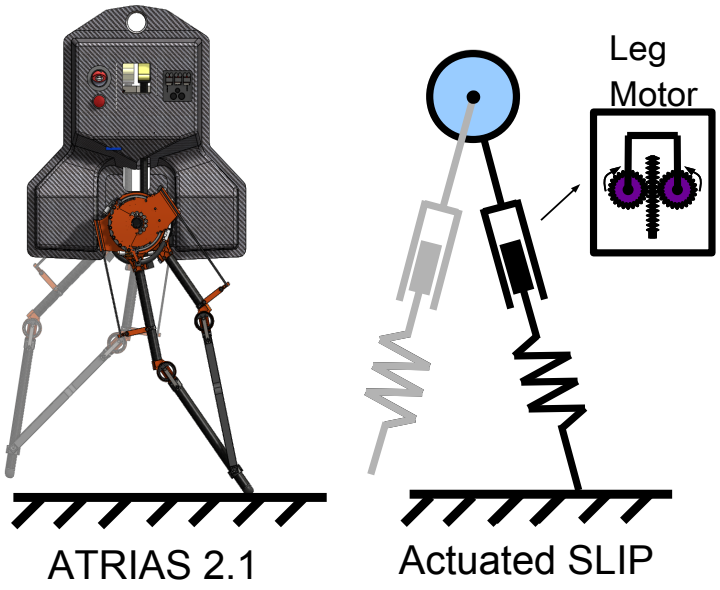

Figure 1.1: ATRIAS 2.1 vs the actuated SLIP model. The leg motor allows the model to change the zero force leg length during the flight phase. The leg is assumed massless and position controller is used for the leg angle placement.

The model that we use in this work is the actuated version of the SLIP model [3] and is mathematically suitable as a simplified model of our robot ATRIAS (figure 1.1). In this model, a motor is used in series with the leg spring to add or remove energy when it is needed to go to higher or lower energy level. All the controllers that we investigate in this study are during the flight phase and therefore, the leg motor is kept locked during the stance phase to provide a passive and conservative gait.

In chapter 2 we propose three control strategies for the flight phase of running. Each of these control policies targets a different objective function to regulate during running and the only control parameter that we use in this chapter is the leg angle at the moment of touch-down. The objective functions are considered for damage

avoidance and energy efficiency, two important technical issues for real robots. We concluded at the end that by implementing either of the proposed control policies in this chapter, both goals will be hit at once with a very simple implementation strategy. After that, in chapter 3, we included the leg length in addition to the leg angle to the control parameters. The aim that we seek in this chapter is to minimize the leg peak force while retaining steady state running in the presence of hidden disturbances. For all of the control policies, we assume that the robot does not have any information of the location and the size of the disturbances, therefore the need for external sensing is minimal. Finally in chapter 4, we derived mathematical formulas for the effect of the characteristics of the passive elements (spring and damper) on the maximum velocity that the robot can achieve in running. To initiate running from stationary position, the motors should add energy to the system and the passive elements can help the robot to reach to a higher energy level. It turned out that both spring and damper can be helpful if they are chosen accurately and if they are not chosen accurately, they both can be harmful to the performance of the system relative to the case that there is no passive element in the system and the motor is directly connected to the body.

The contribution of this work is two types of flight phase control strategies for spring-mass running robots and a mathematical framework for the design of the passive elements for initiating running of these robots. The control policies are easy to be implemented on the machines with minimal sensing. The passive dynamics of the system is used as the main source that drives the system, and the controllers try to manage the balance between the potential energy and horizontal/vertical kinetic

energy. Therefore, the robot theoretically pursues in its original energy level that it started the running in the beginning. For the design of the passive elements of the robot (the physical spring and damper characteristics), we presented mathematical framework that maximizes the achievable velocity at the beginning of running.

Chapter 2 – Swing leg control strategy considering only leg angle

we proposed three swing leg control policies for spring-mass running robots inspired from our recent collaborative work on ground running birds. Previous investigations suggest that animals may prioritize injury avoidance and/or efficiency as their objective function during running. Therefore, in this study we targeted the structural capacity (maximum leg force for the damage avoidance) and the efficiency as the main goals for our control policies, since these objective functions are important to limit the motor size and structure weight. Each proposed policy controls the leg angle as a function of time during flight phase such that its objective function during the subsequent stance phase is regulated. The three objective functions that are regulated in the control policies are i) the leg peak force, ii) the axial impulse, and iii) the leg actuator work. Surprisingly, all three swing leg control policies result in nearly identical subsequent stance phase dynamics. This implies that the implementation of any of the proposed control policies would satisfy both goals (damage avoidance and efficiency) at once. Furthermore, all three control policies require a surprisingly simple leg angle adjustment: leg retraction with constant angular acceleration. In summary, a simple control method (either one of the proposed control policies) satisfies both goals (damage

avoidance and efficiency) at the same time, and it is extraordinarily easy to implement on a machine by providing a constant angular acceleration for the leg retraction.

2.1 Introduction

We seek to understand the principles of legged locomotion and implement them on robots. Recent years have seen remarkable advances in dynamic legged robots, including Rhex, a rough-terrain hexapod [4, 5], Bigdog, a rough terrain quadruped [6], MABEL, a biped that can negotiate uneven terrain [7], ATRIAS, a bio-inspired actuated spring-mass robot [8], and PETMAN a versatile humanoid biped. These robots highlight the emerging potential for legged robotic technology; however each of these machines compete with animal performance and efficiency only within a very limited context. In natural environments animals frequently negotiate potholes, steps and obstacles fantastically. But since we do not yet know how they perform these tasks, we cannot reproduce these behaviors in machines [9]. In this study we seek a reasonable objective function that might be animals concern in running and use it to control the spring-mass running robots. To achieve this goal, we observe the guinea fowl running data (figure 2.1) to gain insights about the goals that they may care during running and then interpret the importance of those goals for real machines. We pick the objective functions that are concerns for current running robots.

There are two reasons we focus on swing leg control: 1. The flight phase determines the landing conditions, which have huge effects on stance dynamics, and

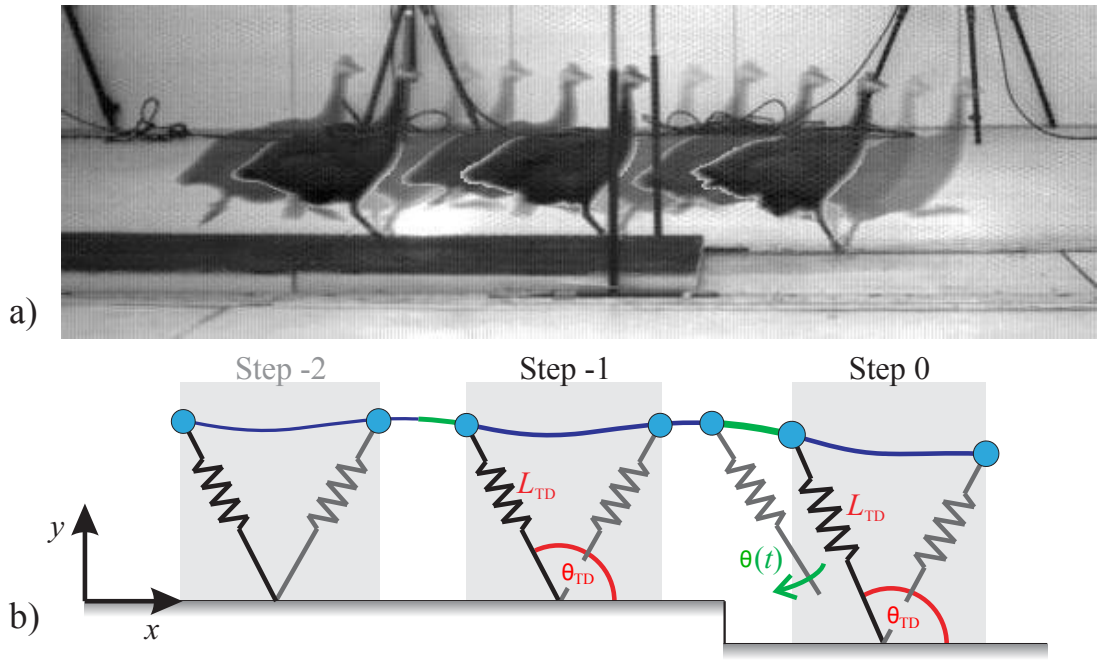

Figure 2.1: Illustration of experiment setup on the guinea fowl running over a step down (a), and schematic drawing of the SLIP model (b). The gray areas indicate the stance phases, and the blue line represents the CoM trajectory [10].

2. adjusting the leg parameters during flight is very energy efficient. The effect of swing leg control methods on the dynamics of a spring-mass system has been investigated in previous literature [11, 2, 12, 13, 14]. From biology perspective, animal running data reveal that the initial leg loading during stance is very sensitive to its landing conditions, which are determined by the flight phase [15, 16, 17, 18]. Daley et. al. [19] showed that for running guinea fowl, variation in leg contact angle explains 80% of the variation in stance impulse following an unexpected pothole. From a roboticist's point of view, swing leg control techniques are energy efficient and easy to implement. Its energy efficiency comes from the fact that there are no

ground reaction forces to overcome during flight to move the leg. Furthermore, using a feed-forward control strategy minimizes the need for sensing, which makes these techniques easy to implement on robots.

Previous theoretical studies of swing leg control suggest a trade-off between objectives like disturbance rejection, stability, maximum leg force and impact losses. For example, a constant leg retraction velocity in late swing improves stability in both quadrupeds [20] and bipeds [12]. Similarly, increasing the leg length in late swing can improve stability and robustness [13]. Whereas low leg retraction velocities improve the robustness against variations in terrain height, high leg retraction velocities minimize peak forces and improve ground speed matching [21, 22]. Alternatively, a feed-forward swing leg control policy can be applied to the spring-loaded inverted pendulum (SLIP) model to maintain steady state running (equilibrium gait), regardless of ground height changes [23]. While maintaining steady state running results in symmetric trajectories even in the presence of ground height changes, it also results in high leg forces and high leg actuator work (electric consumption of the electric motor) during the perturbed step. Karssen et. al. [24] determined the optimal swing leg retraction rate that maximizes disturbance rejection, and minimizes impact losses and foot slipping. They considered a predefined constant retraction rate for running and concluded that there is no unique retraction rate to optimize all of aspects mentioned above at the same time. Especially for high forward speeds, a compromise between disturbance rejection and energy losses is inevitable. Recently, Ernst et. al. [14] demonstrated how leg stiffness may affect the self-stability of a running robot. They proposed a control strategy that updates the leg stiffness based on the fall time

or vertical velocity of the center of mass (CoM).

The equilibrium (symmetric) gait policy is a well-investigated swing leg control policy for spring-mass robots [23, 14]. This policy ensures that the robot's CoM trajectory is symmetric with respect to the vertical axis, which is defined by mid-stance (touch down and take off conditions are symmetrical). Therefore, on flat ground each step is identical to the previous step, resulting in a periodic gait pattern. By choosing the appropriate initial leg angle (touch down leg angle) for each velocity vector $\boldsymbol{v} = (v_{\mathrm{x}}, v_{\mathrm{y}})^T$, a symmetric gait can be obtained. This policy continuously updates the leg angle based on the CoM velocity vector during flight such that whenever the leg hits the ground, a symmetric CoM trajectory is be maintained. In the presence of a drop, however, the required mechanical capacity (leg force for example) can increase drastically, up to the point where the leg may be unable to sustain. Therefore, the equilibrium gait policy may be not a practical control strategy for spring-mass robots.

Inspired by our findings from a previous study on guinea fowl negotiating a drop perturbation [10], we propose three candidates for the objective functions of the swing leg control policies. The objective functions are: i) maintaining constant peak force, ii) maintaining constant leg axial impulse, and iii) maintaining constant leg actuator work. Each control policy adjusts the leg angle during flight such that its objective function during the subsequent stance phase is regulated. The first swing leg control policy ensures that the leg peak force in the following stance phase is the same as the peak force of the previous step. The second policy keeps the axial impulse of the upcoming passive stance phase the same as the axial impulse of the

previous step. The last control policy focuses on economy by maintaining constant electrical work to keep the motor, which is in series with the spring, locked (providing zero mechanical work and thus a conservative passive stance phase). In this case the actuator requires the same electric energy for the drop step and flat ground. We compare these control policies with equilibrium gait policy and against each other.

The results show that the equilibrium gait policy requires more energy and leg force capacity than the other proposed control policies. For economically designed robots that are operating at (or close to) their maximum mechanical capacity, any drop in the ground may cause a damage to the robot or the robot could even fall if the motors are not strong enough. Moreover, it turns out that with a simple swing leg control policy, retracting the leg with constant angular velocity, both goals (optimizing mechanical demand and energy efficiency) could be met at once.

2.2 Bioinspiration

We are inspired by the robust and efficient running of animals. The guinea fowl for example (as dynamical systems) run very agile, robust and efficient in natural environments (uneven terrain). We are looking for control policies that make the legged robots perform as good as animals like guinea fowl in running.

Our strategy is to look at the results from the experiments that have been done in Blum et. al. [10] on the guinea fowl and hypothesize the policies that these birds may follow during running. The experiment setup that they used is shown in figure 2.1.

The experiments showed that the guinea fowl use nearly the same leg length for the drop step as they use for the level running, but the touch down angle for the drop step is significantly steeper than level running. It suggests that the leg touch-down angle may be the only parameter that the guinea fowl use for the flight phase control. Furthermore, processing the force plate data in the stance phase show that the leg peak force and axial impulse during the stance phase are nearly constant for level running and the drop step [10].

2.3 Methods

2.3.1 Model

We consider the spring-loaded inverted pendulum (SLIP) [1, 25] because the passive model of the spring-mass robot is similar to the SLIP model. The actual model of the robot has a leg motor to compensate for the energy loss due to impact and friction (figure 2.2). Since the model is passive in stance phase we do not need the leg motor in our simulation, but its existence can not be ignored. Therefore, we keep the leg motor locked (zero mechanical work) to have a conservative system (like SLIP model in simulation).

The SLIP model is known as a template for studying legged locomotion [26]. This model is based on the ubiquitous behavior of the center of mass that animals have during running. It should be noted that animals and actual spring-mass running robots have leg actuators in series with a spring, but the overall behavior of the system can be approximated well by a passive spring-mass model. Therefore, the

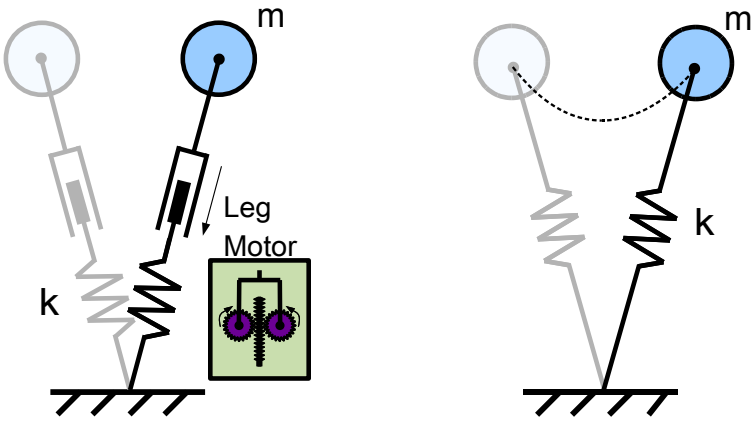

Figure 2.2: left: The model of the robot with the leg motor. The reason of the leg motor existence is to add energy into the system when some energy is lost due to impact or friction. Here, this motor is kept locked (zero mechanical energy) to provide the equivalent conservative SLIP model that is shown in the right.

mechanical energy generated/dissipated by the motors is low, primarily compensating for energy loss, and thus the system can be accounted as a passive conservative SLIP model.

During flight phase of running the CoM describes a ballistic curve, determined by the gravitational force. Therefore, the only parameters of running that can be controlled during the flight phase are the landing conditions for upcoming stance phase. The transition from flight to stance occurs when the landing condition $y = L_0 \sin(\alpha_{\text{TD}})$ is fulfilled. During stance phase the equation of motion for a passive SLIP model is given by

$$m\ddot{\boldsymbol{r}} = k_{\text{Leg}} \left(\frac{L_0}{r} - 1 \right) \boldsymbol{r} - m\boldsymbol{g}, \tag{2.1}$$

with $\boldsymbol{r} = (x, y)^T$ being the position of the point mass with respect to the foot

point, r its absolute value and $\boldsymbol{g} = (0, g)^T$ the gravitational acceleration, with $g = 9.81\,\mathrm{m/s^2}$. Take off occurs when the spring deflection returns to zero. The system is energetically conservative and due to the massless leg there is no impact or friction losses in the system.

The model was implemented in Matlab (R2012a, Mathworks Inc., Natick, MA, USA). To accomplish the simulations, following properties for the robot were assumed.

Table 2.1: Properties of the spring-mass robot

Parameter	**Description**	**Value**
m	robot mass	$38.0kg$
k_{leg}	leg spring stiffness	$3900\frac{N}{m}$
v_{0x}	initial horizontal velocity	$3.5\frac{m}{s}$
h_0	initial CoM height	$57cm$
δ_{gnd}	ground disturbance	$-10cm$

2.3.2 Proposed control Strategies

Inspired by the behavior of birds mentioned in section 2.2, we propose three swing leg control policies. We focus on flight phase control policies because, contrary to stance phase, we can theoretically do no work and still control the gait. Therefore, the controllers would be economically efficient. Leg angle during the flight is the only parameter that would be changed in all the proposed control policies. Each policy controls the trajectory of the leg angle as a function of time $\alpha(t)$ (or vertical velocity) such that the corresponding SLIP model regulates the objective function of the policy in the upcoming passive stance. The objective function for each policy is i)

the leg peak force or ii) axial impulse or iii) the leg actuator electric work. Therefore, each control policy tries to find the appropriate leg angle during the flight phase at each instant to keep its objective function the same as previous stride. When there is no disturbance in the ground (level running), all of these control policies lead to equilibrium gait policy.

We assume that our model has no information about the location and the size of the drop perturbation, and the leg angle is adjusted continuously starting at the instant of the expected touch down in anticipation of ground contact. Therefore, on flat ground, equilibrium gait is obtained and on a drop step, the leg angle would be adjusted at each instant such that the objective function is regulated for the stance phase. It should be noted that no control is applied during the stance phase and it is purely passive.

2.3.2.1 Constant peak force policy

The first proposed control strategy is to regulate the peak force during running. This control policy adjusts the leg angle during the flight phase such that the resulting leg peak force in any drop step remains the same as it used to be during the level running. This control policy makes it possible for the running robots to operate at their maximum capacity on even terrain and relinquishes the need to reserve some of the mechanical capacity for the drop step (unless the leg would break) and hence yields to a lighter and more efficient robots. Also, observations from birds' data show that they run at nearly the same peak force during the level running and drop step

([10]). It should be noted that the controller does not need to have any information about the size and location of the drop (minimal sensing), in this policy the leg angle is adjusted continuously during the flight phase such that the leg peak force gets regulated.

In the presence of a drop, the leg angle retracts towards the ground. Contrary to equilibrium gait policy, as indicated in appendix 2.7, for constant peak force policy the leg always should retract to fulfill its objective function. This behavior helps to reach the ground sooner and hence prevents the vertical velocity from increasing more. The reason that the leg is retracted before hitting the ground in this control policy is as follows: As the robot falls, the vertical velocity of the CoM increases and consequently the velocity vector rotates towards the leg. To avoid the increase of the peak force, the angle between the velocity vector and the leg direction should be increased. To increase this angle, the leg should be retracted even faster than the rotation of the velocity vector towards the leg. This implies the retraction behavior for the leg.

2.3.2.2 Constant axial impulse policy

The axial impulse is another objective function that we propose to be regulated during the running. We picked the axial impulse because this function considers both leg force and the leg work at the same time (our both goals), keeps consistent energy storage in the spring and also is able to reproduce the observed animal behavior. Constant leg impulse control policy provides the same axial impulse for the drop

step as for the level running by only adjusting the leg angle during the flight phase. This control policy - like the constant peak force control policy - retracts the leg at the presence of the drop perturbations, to retain the axial impulse the same as the previous step.

The mathematical formula for the axial impulse is:

$$I = \int_0^{t_s} F \, \mathrm{d}t$$

In the above equation, F is the force in the leg direction and t_s is the stance time.

2.3.2.3 Constant leg work policy

In this section we regulate the actuator work during the running process. Although the experimental data from birds' running shows very slight change in the magnitude of the peak force or axial impulse in drop step respect to level running, these changes are statistically significant (low standard deviation in the data). It means these values (leg peak force and axial impulse) definitely change in the presence of the drop step, but not significantly in magnitude. In this section we investigate regulating another criteria that directly targets the efficiency of the system. The presence of the muscles in series with tendons in animals is similar to the presence of the motor in series with the leg spring for running robots. We know that electric motors consume electric energy even when they are kept locked. It means although the whole system remains energetically conservative and the generated/consumed mechanical work is zero, but the leg actuator needs electric energy to stay locked.

To regulate the electric work for this control policy in the drop step, the leg angle should be adjusted such that the leg actuator electric energy be the same as it used to be for level running. Since the electrical energy consumed by electric actuators is proportional to the integral of the torque squared over stance time, we use this integral as the criteria for the consumed electric energy. The mathematical formula for the electric work criteria is defined as:

$$W = \int_0^{t_s} F^2 \, \mathrm{d}t$$

This control policy - like the two previous control policies - retracts the leg in the presence of the drop step to keep the leg actuator work constant and consequently, like before, this behavior helps the leg reaches the ground sooner because of the steeper leg angle at the time of the touch-down.

2.4 Results

In this section we investigate, in simulation, the success of the control policies in the presence of a hidden drop step and then, compare the three proposed control policies against the equilibrium gait policy (Appendix) and against each other. Since the system follows its passive dynamics during the stance phase, the difference in the behavior of the system for each policy comes from the different touch-down angles.

Figure 2.3 shows the CoM trajectories for one step before the drop and the drop step. Since the robot does not have any information about the disturbed step, the step before the drop would be the same as level running. All the control policies

could successfully pass the drop step and the robot didn't fall. The overall shape of the CoM trajectories during the drop step are very similar for the three proposed control policies and clearly different from the equilibrium gait policy. The constant force control policy touches the ground slightly sooner than the other two policies and hence leaves the ground with a lower height and less vertical velocity.

The CoM trajectories in figure 2.3 imply that the robot accelerates horizontally in the drop step for all the three proposed control policies, but for equilibrium gait policy the robot maintains the same forward speed as before. It should be noted that although part of the potential energy of the system is redirected to the horizontal kinetic energy, but since the velocity is with power two in the kinetic energy, the resulting horizontal velocity after the take-off does not increase too much especially for high forward speeds. For example, if the initial forward speed is $5m/s$, after redirecting the change in potential energy from falling of a $20cm$ drop to horizontal velocity, the resultant forward speed will be $5.4m/s$. It means only 8% increase in the forward speed after the $20cm$ drop.

The leg force profiles are shown in figure 2.4. The leg peak force in the drop step for equilibrium gait policy increases about 45% of the level running while for the proposed control policies it remains nearly the same as before. The leg peak force increases slightly for the constant impulse and constant work relative to the constant peak force policy, which is the same as level running.

The axial impulse would decrease for the constant peak force and constant actuator work policies in the drop step (figure 2.5), but it increases about 60% for equilibrium gait policy.

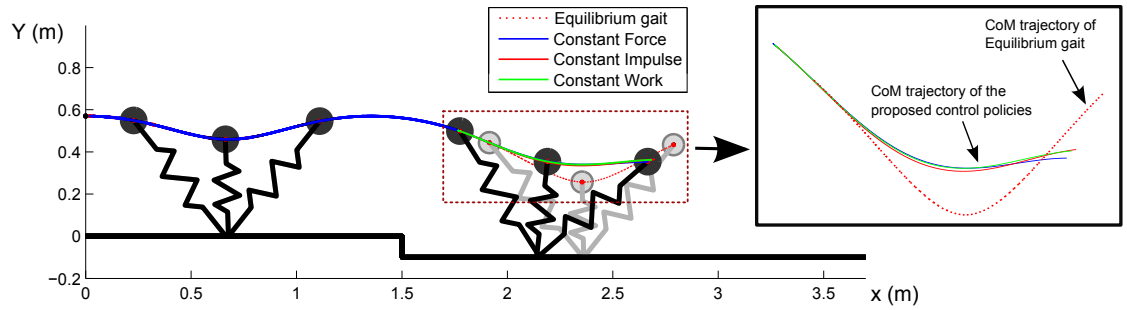

Figure 2.3: CoM trajectories of the robot subjected to the three proposed control policies and equilibrium gait control policy. For the proposed control policies the height of the CoM is lower at take-off respect to touch-down and equilibrium which implies that the system would have higher forward speed at take-off. This is the same behavior that we observe from animals.

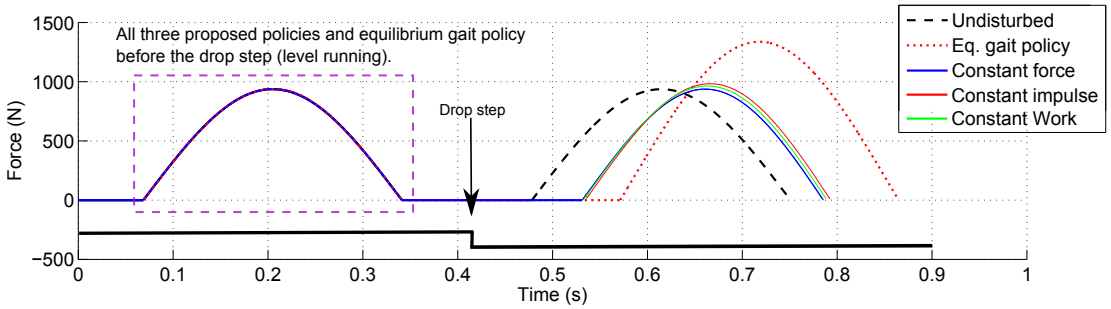

Figure 2.4: Axial force profiles for the three proposed control policies and the equilibrium gait control policy and undisturbed situation. The peak force in equilibrium gait control policy increases about %45 respect to the undisturbed peak force. The beginning of the force profiles show that the equilibrium gait policy reaches the ground the last.

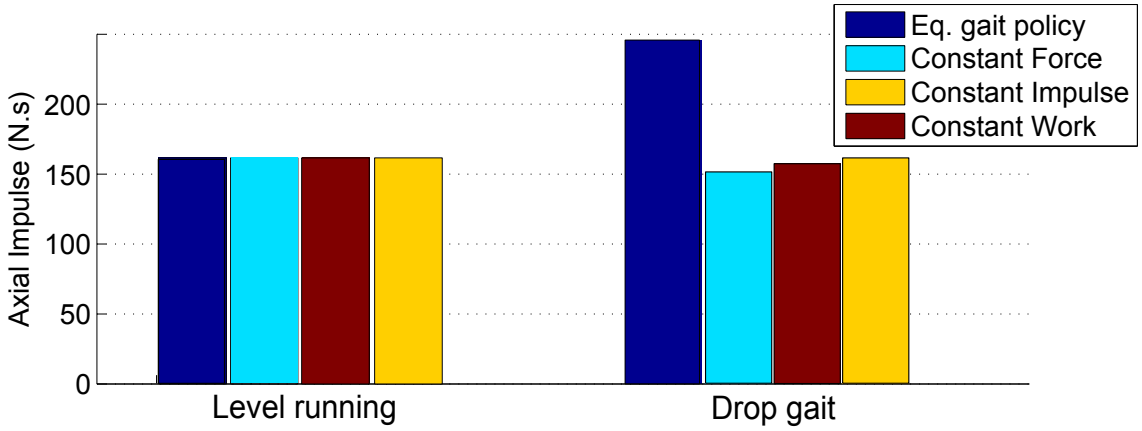

Figure 2.5: Axial impulse in the leg during the stance phase for level ground and drop step. The axial impulse for drop step with equilibrium gait control policy is much higher than the level running. For the constant peak force and constant work policies, the axial impulse in drop step decreases a little bit respect to the level running.

Figure 2.6 compares the efficiency of the control polices from the required electric energy point of view. The constant axial impulse policy requires 7% more electric work for the drop step than level running, but the constant force needs the least electric energy in the drop step (about 5% less than level running). While the proposed control policies require nearly the same amount of electric energy for the drop step as level running, the required electric energy for the equilibrium gait policy at the drop step is more than 2 times of the energy that the actuator needs for level running.

Figure 2.7 compares the touch-down angles for each control policy and show qualitatively how the objective functions change in difference scenarios. In this figure the proposed control policies are depicted on the peak force, impulse and leg work contour lines. moving along each contour line means following the corresponding

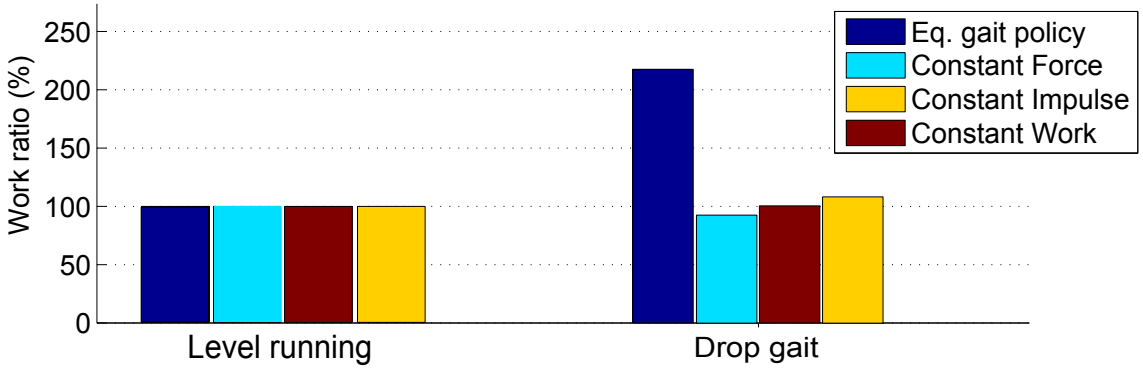

Figure 2.6: Actuator electric work criteria to keep the motor locked during the stance phase. The required work for drop step with equilibrium gait control policy is much higher than the level running (more than 2 times), but the required electric work with constant peak force control policy is nearly the same as level running.

control policy. During the level running, all the proposed control policies and the equilibrium gait policy coincide at one point (it is shown with the gray big circle in the figure). The small colored circles show the touch down condition of the robot following each of the control policies at the drop step. As the vertical velocity increases, the contour lines diverge from each other, which implies more different behavior from the system under each control policy.

The shapes of the contour lines in figure 2.7 are close to linear for small changes in vertical velocity. To study the shape of the contour lines further, we focus on only the peak force contour lines in figure 2.8. This figure shows the desired leg angle trajectory, which is the same as the peak force contour lines, and two sets of fit, linear and quadratic function, for the desired leg angle trajectory. The linear fit of the desired leg angle trajectory has drift along the desired curve, and this drift gets

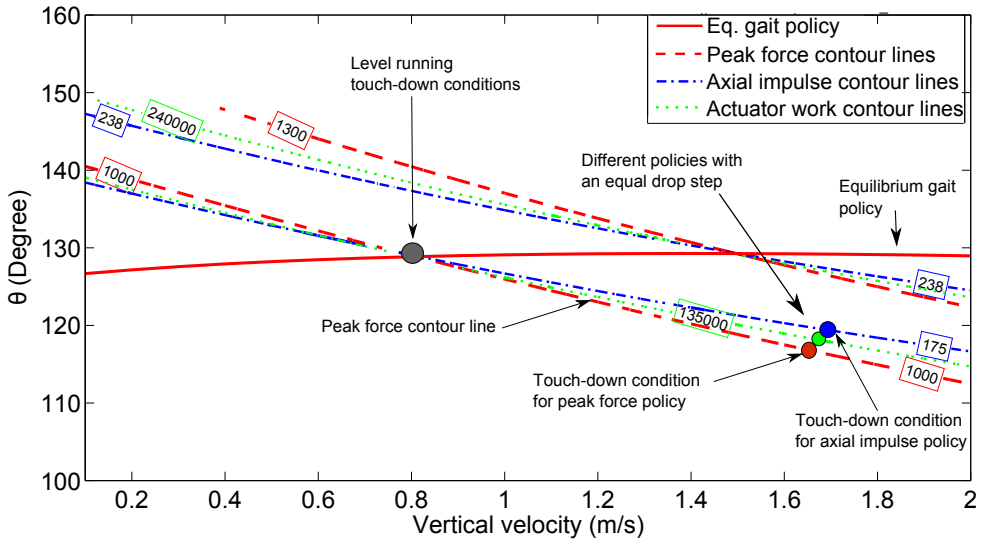

Figure 2.7: Contour lines for leg peak force (red), axial impulse(blue) and leg actuator electric work(green). The big gray circle shows the level running touch down condition and the small colored circles show the touch down angle at the drop step following each of the control policies. Since the contour lines are close to linear respect to vertical velocity (or time), a constant angular rate for the leg retraction would be a good approximation for the policies.

smaller as the forward speed increases. The quadratic function is an excellent fit for the leg angle update.

2.5 Discussion

All the proposed control policies are able to reject the drop step with a similar behavior. Therefore, each of them individually has the capability to be used as a swing leg control policy and by implementing either of them, the other two policies would be nearly fulfilled as well. Among these policies, the constant force policy leaves the ground with a lower height and less vertical velocity which means, it has the shortest flight phase after leaving the ground to adjust the leg for the next stride, the constant impulse and constant work control policies have nearly the same flight phase time and slightly more than constant peak force policy. For the equilibrium gait policy [23, 14], the CoM trajectory remains symmetric and the robot would have the largest flight time to be prepared for the next step.

Results show that the equilibrium gait policy in the drop step requires much more demands (mechanical (leg force) and electric energy) than the proposed control policies. The 45% increase of the leg force in the results section may lead to serious structural damage to the leg, and even if the structure of the leg can sustain this new force, the amplifiers may not be able to provide that much current and hence leads to falling. For the proposed control policies, on the other hand, the internal demands remain nearly the same as before. For example the leg peak force increases slightly (about $2-3\%$) for the constant impulse and constant work relative to the

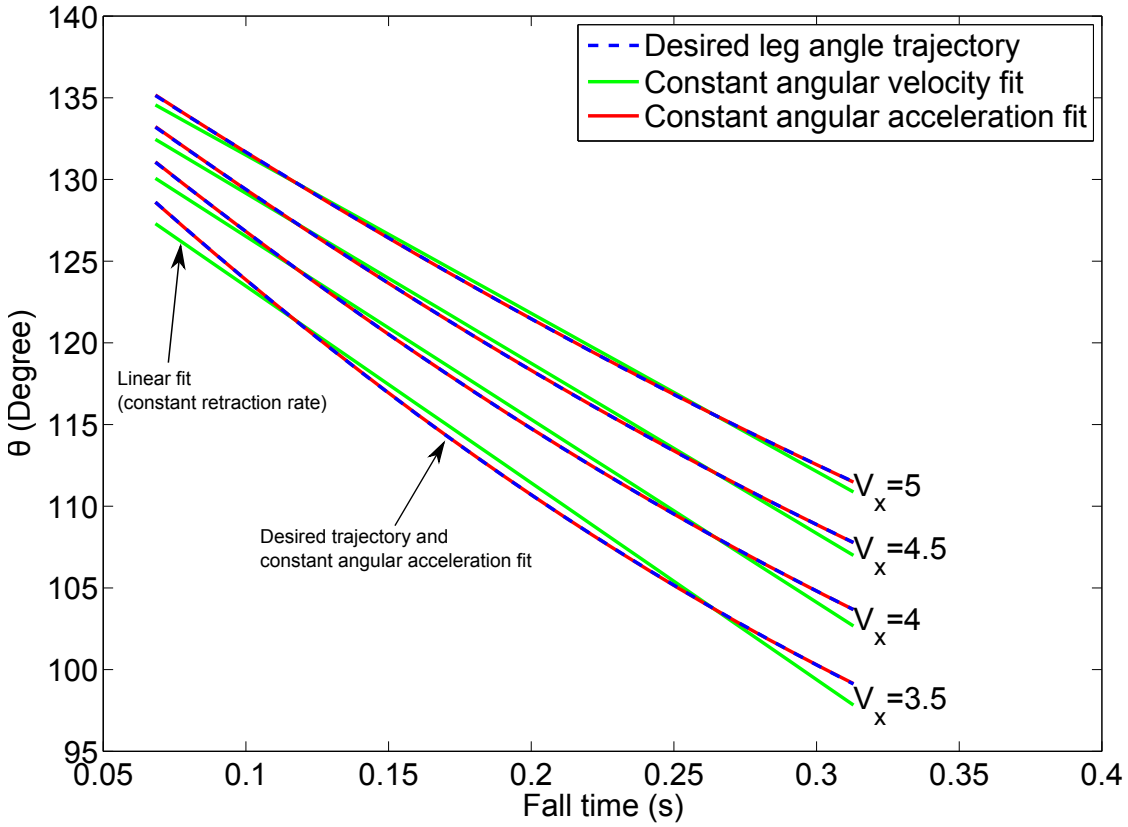

Figure 2.8: Desired and fit functions for the leg angle trajectory subjected to the constant peak force policy. The blue dashed lines are the desired leg angle trajectory and the green solid lines and red solid lines are linear and quadratic fit respectively. The constant angular acceleration fits the exact desired trajectory very well. As the forward speed increases, the constant retraction rate approaches the exact desired trajectory. The value for the retraction rate can be obtained from the slope of the contour lines.

constant peak force policy, which is the same as level running.

The asymmetric shapes of the CoM trajectories in the proposed control policies during the drop step imply that the robot accelerates horizontally in the drop step for all the three proposed control policies. This is consistent with the behavior that animals show in the drop step [10]. But for equilibrium gait policy, the robot maintains the same forward speed during the whole running. The increase of the horizontal velocity in the drop step for the proposed control policies is due to the conversion of the potential energy (from drop height) to the kinetic energy. Since the velocity is with power two in the kinetic energy, the resulting horizontal velocity after the take-off does not increase significantly, especially for high forward speeds. For example, if the initial forward speed is $5m/s$, after redirecting the change in potential energy from falling of a $20cm$ drop to horizontal velocity, the resultant forward speed will be $5.4m/s$. It means the forward speed increases only 8% after falling from the $20cm$ drop.

The proposed control policies here consider the mechanical and electrical limitations as the central concern for the controllers. Other preferred requirements like the next stride apex height and apex horizontal velocity are in the second priority of the control policy and can be determined similar to the dead-beat control strategies [27, 23] or the Raibert controller [28]. Later in this section we will discuss more about these aspects.

Since the shapes of the contour lines in the leg angle (θ)-fall time (t) plane (figure 2.7) is close to linear, a constant leg retraction rate with the average slope of the contour lines would be a simple implementation strategy. The value for the leg

retraction rate agrees with Karssen et. al. [24]. Further investigation in the shape of the contour lines revealed that constant leg angular acceleration is an excellent fit for the swing leg retraction trajectory. As the horizontal velocity increases, the linear function becomes more acceptable fit for the contour lines. Therefore, for high forward speeds (forward speed more than $6m/s$), constant leg retraction rate is nearly the same as the slope of the contour lines and hence is nearly exact. Among the contour lines, the peak force contour lines have the steepest slopes which means the greatest leg retraction rate among other policies.

The objective functions that we chose for the policies are important technical issues from the robotics point of view. We tried to find an exact map that regulates our objective functions, but surprisingly the map function happened to be a simple constant leg angular acceleration. For small flight time (falling from small drop heights), constant leg angular velocity is a good approximation for this map. The outcomes agree with what Karssen et. al. [24] found for the optimal swing leg retraction rate when the peak force is considered as the objective function. But contrary to their work, we did not limit our policy to a constant leg retraction rate.

The difference between the proposed control policies and the equilibrium gait policy increases as the forward speed increases. To provide steady state running for high forward speeds, the leg should protract in the falling half of the flight phase (appendix), but for all the proposed control policies the leg should retract to reach the ground. The leg protraction in the equilibrium gait policy postpones the moment of the touch-down and consequently increases the difference of the proposed control policies and the equilibrium gait policy. Karssen et. al. [24] also reported that the

trade-off between optimal swing leg retraction rate for the disturbance rejection and other objective functions (including the leg peak force) increases by increasing the forward speed.

The desired leg angle trajectory for each of the proposed control policies is different with the two-phase constant leg retraction rate in the clock-driven model that was proposed for the robots like RHex [4] [5] [29]. In each of the proposed control policies, Like the clock-driven model, the leg retraction trajectory after the time of the expected touch-down would follow a different trajectory function. But in these policies, instead of a constant retraction rate, constant angular acceleration should be provided for the leg, and more importantly, contrary to clock-driven method, the control efforts stop at the beginning of the stance phase (contrary to clock-driven technique, proposed control policies are purely passive in stance phase). The clock-driven technique is a simple bio-inspired technique, but it does not consider the structural or electrical capacity of the leg and hence these technical issues may cause damage during the stance phase.

By using a new type of return map, the proposed control policies and their limitations can be depicted visually. In this new type of return map, contrary to return maps with constant mechanical energy [2, 14], the horizontal velocity is kept constant (figure 2.9). In the return maps with constant energy, any change in the ground level alters the energy of the system and therefore, the flight phase control policies with varying ground level can not be depicted on the maps (figure 2.9-a). In the return map that we use here, instead of the mechanical energy, the horizontal velocity is kept constant (figure 2.9-b). The key difference of these two return maps

is: the axes in the return map with constant mechanical energy represent the apex heights relative to the original ground level, but in the return map with constant forward speed, the two axes are the apex heights relative to the upcoming stance phase ground level. In figure (2.9-b), y_i represents the apex height relative to the upcoming stance phase. Therefore, any change in ground height is interpreted as the change in y_i (for example if there is a $10cm$ drop step, then this apex height increases $10cm$). The vertical axes of this graph (y_{i+1}) is the apex height relative to the upcoming stance ground level.

To implement the constant peak force control policy, the leg angle should follow parallel to the axial peak force contour lines. Using the constant forward speed for this map allows us to interpret the change of the ground level as a change in the apex height. Therefore, contrary to the conventional return map [2, 14], we do not need to change the graph. For example, if the apex height for steady state running is about $57cm$ then the peak force would be $1000N$. Now assume the drop height is $10cm$ therefore the apex height including the drop step would be $67cm$. To follow the constant peak force policy, the leg angle should be set to $\theta = 121^\circ$ at the moment of touch-down, and the passive dynamics of the system drives the stance phase and has the same axial peak force as before ($1000N$). It should be noted that there is no need to know the ground level in advance and the leg angle is getting updated continuously expecting to reach the ground at that moment. To have steady state running (equilibrium gait policy), the controller should follow the 45° line which requires the touch down angle be about $\theta = 129^\circ$ and consequently the peak force in the leg surges to about $1350N$ (35% increase). Also, we can notice that although the

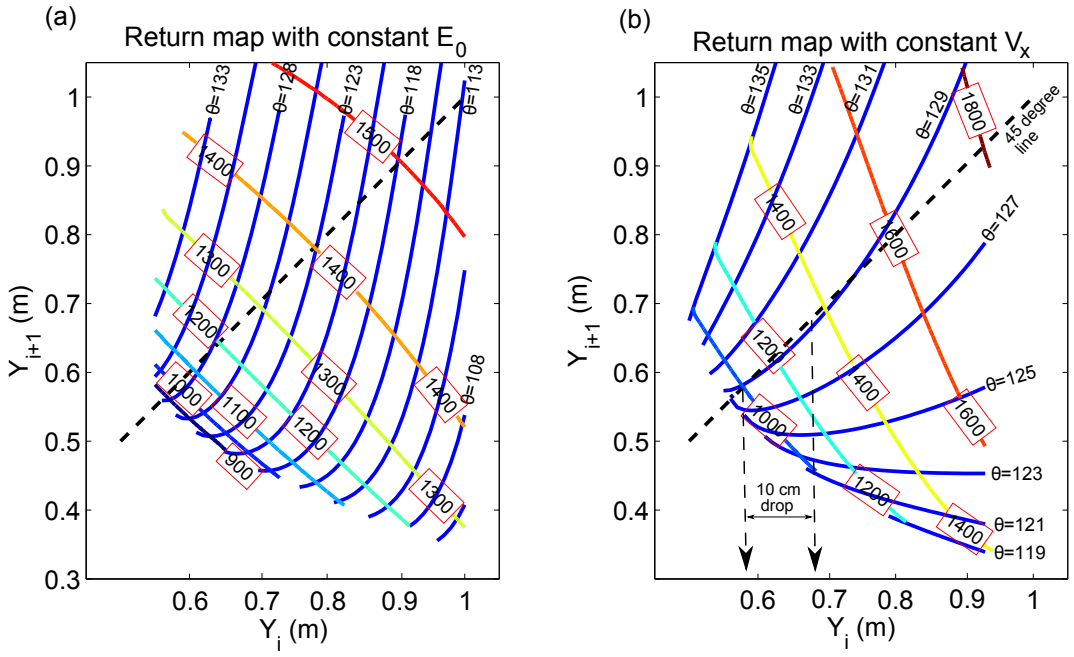

Figure 2.9: Return map with constant mechanical energy ([2, 14]) (a) and return map with constant horizontal velocity (b). There are two sets of contour lines: leg angle (θ) contour lines [Degree] and axial peak force contour lines [N].

constant peak force policy prevents the peak force from increasing, it has a limit for the maximum drop height that can be handled by this control policy. For example, to keep the peak force equal to $1000N$, the maximum drop height that can be handled is around $10cm$ (the end of the $1000N$ contour line). It implies that for deeper drop steps, the peak force would increase unless the robot does not leave the ground after the passive stance phase.

Because of the negative slope of the force contour lines in the return map, the next apex height decreases with increasing the drop height. It implies that the system gains horizontal velocity due to the transformation of the potential energy to kinetic energy. This behavior is confirmed in simulation and also observable from animals' experiment [10]. Also, we know that to have a successful running gait, the next apex height is another important factor that should be considered. The next apex height after the drop step should be greater than a threshold and the flight phase should be long enough to allow the leg to be placed on the ground for the next stride. Therefore, based on the geometry of the leg, the controller should limit the allowable drop height, or use a shorter leg length for the next stance phase. For all these cases, the return map with constant horizontal velocity can determine the limitations and one can design the appropriate scenario for the control policy on the map.

The discussion of the return map that we presented for constant peak force policy, can be easily extended for axial impulse or leg work. In these cases, only the peak force contour lines in figure 2.9 would change to the impulse or leg work contour lines in the range of $175N.S$ to $300N.S$ and $135000N^2.S$ to $350000N^2.S$ respectively. The overall shape of the impulse/leg work contour lines are similar to the peak force

contour lines in figure 2.9.

It should be remembered that all the proposed control techniques were during the flight phase and the system was assumed conservative during running. Therefore, to continue running on ground with a permanent drop step, the robot should dissipate the gained kinetic energy. In this case, a stance phase control is inevitable to return the robot back to the preferred forward speed unless the robot will continue with a higher horizontal velocity. A simple and bio-inspired stance phase technique that was proposed by Schmitt et. al. [30] and investigated more by [31] and [32] can be used to dissipate the gained energy.

2.6 Conclusion and future work

Three flight phase control policies inspired by animals' data, but suitable from mechanical perspective for machines, were proposed and implemented to the model of spring-mass running robots. The control policies regulate their objective functions that target the mechanical/amperage limitation and electrical efficiency of the system. Therefore, by using either of these bio-inspired control policies, the safety and efficiency of the robot during running is guaranteed while we showed that the implementation of them is very easy with minimal sensing requirements.

All the three proposed control policies (constant peak force, constant axial impulse and constant leg actuator electric work) successfully rejected the drop step and surprisingly resulted in similar behavior on the spring-mass robot. Therefore, by implementing either of these proposed control policies, both goals (damage avoid-

ance and efficiency) would be satisfied. For instance, by implementing the peak force control policy (which was considered for damage avoidance and amplifier limitation) the efficiency goal would also be achieved.

We showed that a simple leg angular acceleration during the flight phase is enough for the robot leg to keep the running safe (avoiding the damage) and efficient. If the drop height is less than 10% of the leg length, a constant leg angular velocity (constant leg retraction rate) would approximately give similar results. The value of the leg retraction rate (leg angular velocity) can be found from the slope of the leg peak force contour lines in the leg angle-falling time plane. It should be noted that implementing these policies are very easy and requires very little sensing or computation on a robot.

For future work we plan to implement these policies on our robot ATRIAS. We found out that the amperage limitation is a big concern for actuated spring-mass robots like ATRIAS and therefore, we will start with the constant leg peak force policy.

2.7 Appendix: Equilibrium gait policy

The equilibrium gait policy ensures that the robot has symmetric CoM trajectories during the stance with respect to the vertical axis defined by mid-stance (i.e. touch down and take off conditions are symmetrical). To create symmetric gait for high forward speeds in the presence of a drop, the leg should protract as the CoM falls in the drop (figure 2.10). This protraction opens more room between the toe and the

ground and consequently leads to higher vertical velocity at the time of touch down. To have equilibrium gait, figure 2.10 shows the leg angle function with respect to falling time for different forward speeds. For low horizontal velocities, the leg angle function is monotonically decreasing meaning that the leg should be retracted after passing the apex. For high forward speeds (here $v_x > 3$) the robot should protract the leg in the beginning and then (after gaining some downward velocity if it yet hasn't reached the ground) it should start retracting the leg to provide the appropriate leg angle for equilibrium gait. For human-scale spring-mass running robots, high downward velocity (here more than about 2 m/s which corresponds to a drop height of about 30% of the leg length) is not common to be rejected blindly. Therefore, for small to medium drops, the leg would have monotonic behavior. It is interpreted as retraction for low forward speeds and protraction for high horizontal velocities as the robot falls.

Karssen et. al. [24] also concluded that for high horizontal velocity, the trade off between the disturbance rejection and energy losses and also foot slipping increases. The reason is that when the forward speed is such that protraction is needed, the leg should be rotated in the opposite direction of falling, but to reduce the effect of impact or prevent the foot slipping the leg should be retracted (it should be rotated in the direction of falling). Moreover, as the robot falls, the protraction increases the distance between the toe and the ground and postpones the contact moment, meantime the vertical velocity increases and consequently the leg peak force or axial impulse increase more.

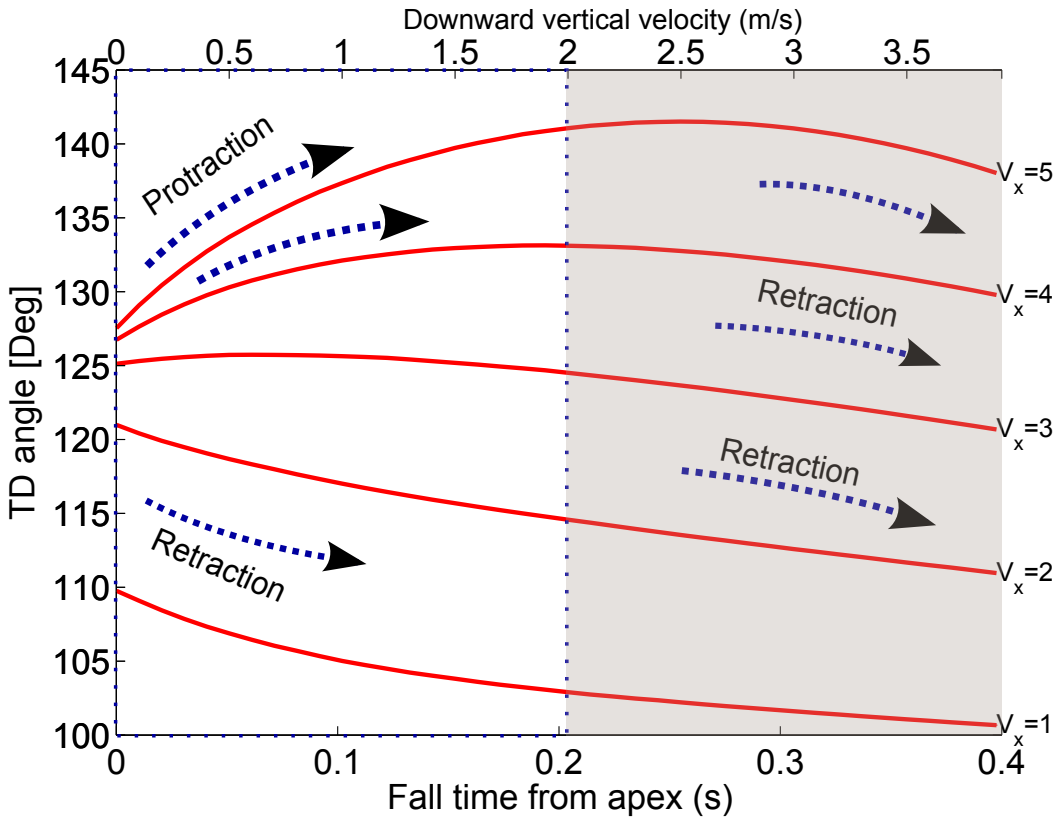

Figure 2.10: The required leg angle trajectory for equilibrium gait policy. For low horizontal velocities, the leg should be retracted as it falls. For high forward speeds (here about $v_x > 3$) the robot should protract the leg in the beginning and then it should start retracting the leg. The shaded area corresponds to deep drops (disturbances more than about 30% of the leg length that is not very common for legged robots to reject blindly.

Chapter 3 – Swing leg control strategy considering leg length and leg angle

In this paper we present a control strategy for spring-mass running robots that maintains a consistent running gait on uneven terrains, while prioritizing a limit on the peak forces on the leg. The peak forces are a problem for real machines, potentially exceeding the peak forces of an actuator and leading to a fall, or even breaking robot components. Our control strategy relies on an actuated spring-mass model which is described in section 3.2. Our controller chooses a leg angle and a leg length during the flight phase, relying entirely on passive dynamics during the stance phase to have symmetric gait and not suffer from high leg forces during the stance phase.

3.1 Introduction

The planar spring loaded inverted pendulum (SLIP) has been widely used in literature as a model for walking [33, 11] and running [1, 23]. The stability of this simple model in running [34] explains how animals can run robustly and efficiently in real world. Schmitt et. al. [30] added a very simple controller to the passive SLIP model and made the system more robust.

Recently Ernst et. al. [23] proposed a flight phase control strategy for running

on uneven terrain that leads to steady state running. In their method, the leg angle is chosen such that a steady state running is produced during the stance phase. This control strategy does not require any work during the stance phase, but the leg force is increased dramatically.

Our motivation for this study comes from the response of animals to hidden disturbances [35] as is shown in Figure 3.1. For them, too, peak leg force appears to be a concern. Ground-running birds carefully limit their leg peak forces when encountering unexpected drop perturbations by extending their legs and adjusting their leg angles[35] (Figure 3.1).

Inspired by the behavior of animals in running, we intend to investigate the effect of the leg length on the dynamics of running. Therefore, a leg actuator is added to the SLIP model [3] to control the length of the leg during the flight phase (Figure 3.2). The observation of animals' behavior shows that in the level running, the CoM trajectory is close to a symmetric path. When they encounter hidden drops in the ground, their leg length increases to fill the unknown hole height and their leg angle is adjusted to reject the disturbance robustly and efficiently. The steady state running (equilibrium gait) for the SLIP model can be obtained when the leg touch-down angle is the same as the leg lift-off angle and also the CoM velocity components are the same.

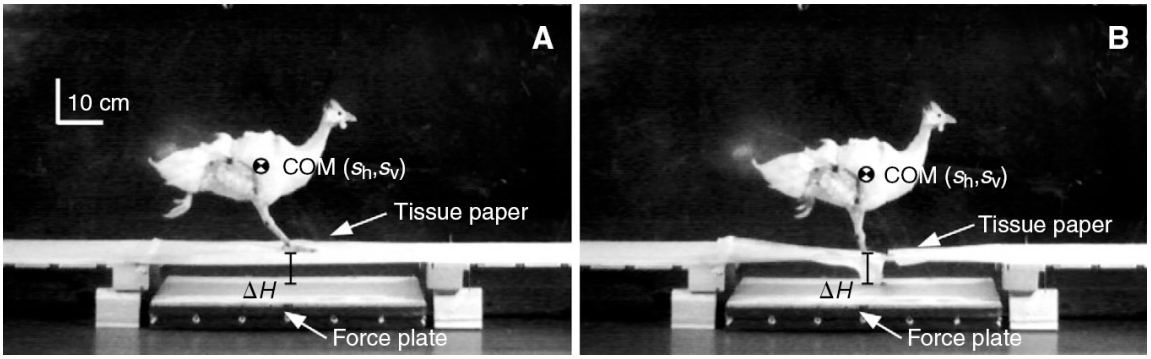

Figure 3.1: By extending their leg length and adjusting their leg angles, guinea fowls reject hidden disturbances without suffering from high leg forces[35].

3.2 Methods

3.2.1 Model

The model that we use here is an actuated version of the SLIP model [3] which is shown in Figure 3.2. The leg actuator is in series with the spring to control the leg length during the flight phase. We keep the motor locked during the stance phase, therefore the dynamics of the system will be entirely passive (SLIP model) in stance phase. The motor inertia and maximum motor torque are considered for the leg actuator to model a realistic electric motor. In addition to the leg length control we assume, like previous studies [23, 34, 30], that the leg angle can also be controlled during the flight phase. The leg angle is controlled with position control technique.

For real robots, any leg mass can be included in motor inertia. In this case, the important physical limitations are considered in the results. To accomplish the simulations, following characteristics are chosen for the model.

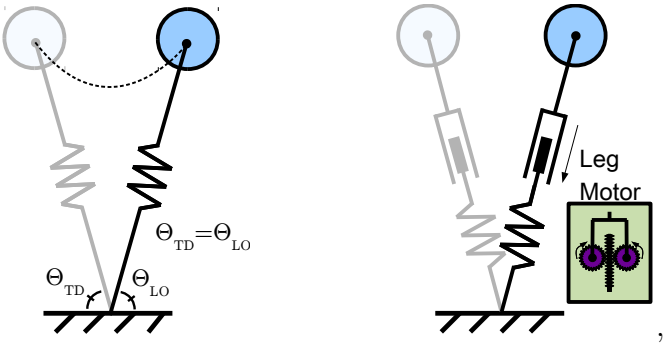

Figure 3.2: The passive SLIP model vs. the actuated SLIP model.

Table 3.1: Robot characteristics for one legged robot

Parameter	**Description**	**Value**
m	robot mass	$30.0kg$
k_{leg}	leg spring stiffness	$4500\frac{N}{m}$
l_0	initial spring length	$70cm$
T_{max}	maximum motor torque	$850N.m$
I	motor inertia	$2.78kg.m^2$
G	Gear ratio	$50:1$
v_{0x}	initial horizontal velocity	$2.5\frac{m}{s}$
h_0	initial CoM height	$70cm$
δ_{gnd}	ground disturbance	$-15cm$

3.2.2 Control strategy

The main goal of this control strategy is to keep the equilibrium gait during the running. Previously, Ernst et. al. [23] proposed a method to have equilibrium gait (steady state running) by only adjusting the leg angle during the flight phase. Based on their control strategy, the leg angle during the flight phase should be continuously updated, as a function of fall time, such that if the toe reaches the ground at each moment, the passive dynamics of the system will create the equilibrium gait. Figure 3.4 shows the CoM trajectory of the SLIP model with this control policy. To imple-

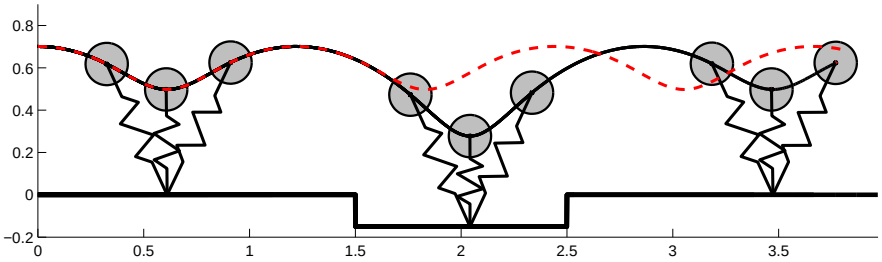

Figure 3.3: CoM trajectory of the SLIP model adjusting the leg angle with constant leg length to have symmetric gait (equilibrium gait policy) [23].

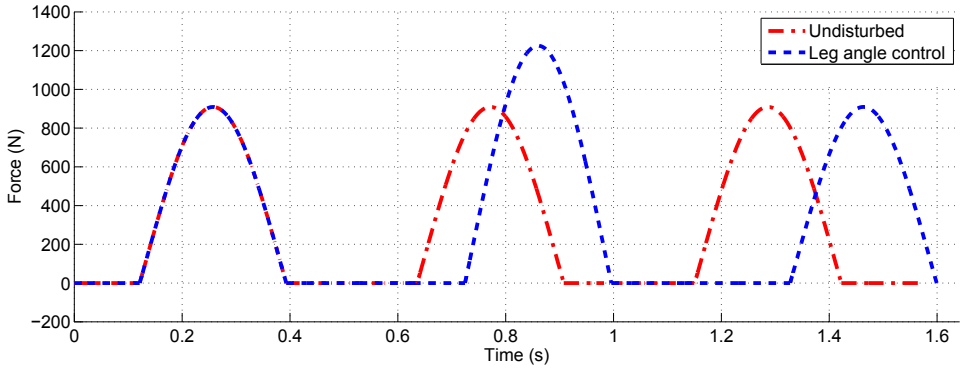

Figure 3.4: Leg force profiles for the undisturbed model and the equilibrium gait policy. The leg peak force increases about 33% for the equilibrium gait policy.

ment this control policy on a real robot, we need to generate a look-up table which gives us the appropriate touch-down angle with respect to the vertical component of the CoM velocity. The main problem with this control policy is that the peak leg force during the pothole step increases significantly. Simulations show that the increase in the peak force in drop gait is about 33% of the level running value. This increase may break the leg or the transmission of the robot. It should be noted that the increase in the leg peak force would be more pronounced for higher forward speeds.

The control policy used by animals uses the leg extension in addition to leg retraction. Therefore, at each instant (means constant vertical velocity during the flight phase) we look for the relation between the leg length and the leg angle that leads to a symmetric gait for SLIP model. Moreover, we monitor the change in the peak leg force in the stance phase. We need to expand the previous look-up table that Ernst et. al. [23] proposed. In the new look-up table different leg lengths should also be included. Therefore, the required leg angle in each instant is obtained based on the falling time (or vertical velocity) and the current leg length by interpolating among the look-up table data. Since the system is purely passive in stance phase, the well known SLIP model equations of motion are used in stance phase [11, 30].

In Figure 3.5 the relation between the leg length and the leg angle is shown for different vertical velocities to have equilibrium gait. Each point (pair of leg angle and leg length) on the lines leads to an equilibrium gait for the corresponding vertical velocity. The numbers on the curves show the peak leg forces at those points. It can be seen that to have symmetric gait, the peak force is nearly constant for different leg lengths (numbers along each curve in Figure 3.5). It means if the leg length extends while the leg angle is being adjusted concurrently (like animals do), the peak force in the stance phase does not vary too much. The whole point is that the leg extension compensates for the hole height and therefore, a symmetric path with nearly constant peak force is generated during the stance phase.

In summary we can design the controller as follows: if the vertical velocity passed the usual value at touch-down; the leg actuator should extend the leg towards the ground. Based on the current leg length at each moment the leg angle should be

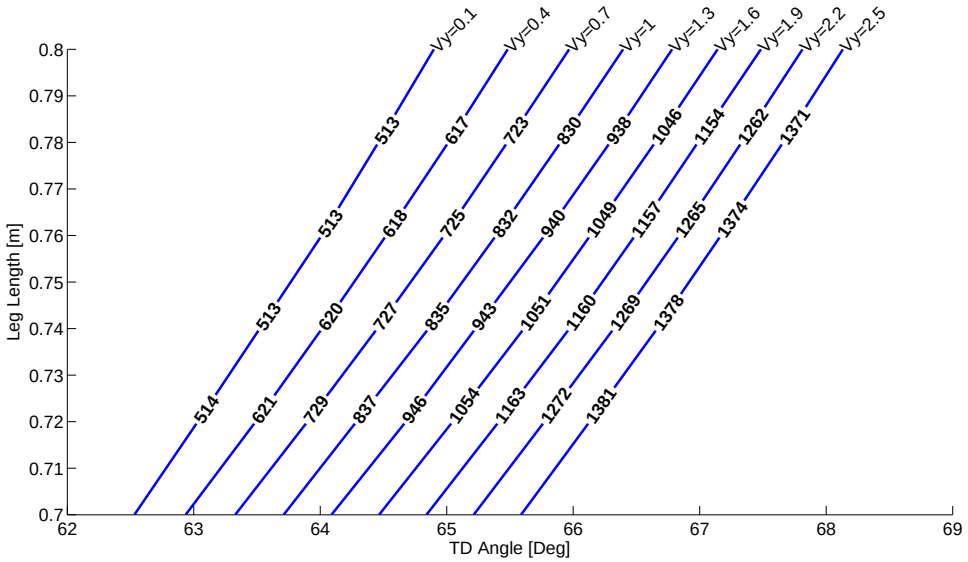

Figure 3.5: Leg length vs leg angle for equilibrium gait policy with different vertical velocities. Numbers on the lines show the peak leg force [N] during the stance phase at that point. The peak forces are nearly constant along each curve.

adjusted using the curves in Figure 3.5 or the look-up table that was mentioned earlier.

Two different scenarios that may happen during the running are shown in Figure 3.6. When the vertical velocity of the CoM is less than or equal to the usual value of the vertical velocity at touch-down, the motor does not work and only the leg angle is adjusted to generate symmetric path in stance phase (if there is any step up in the ground). If the vertical velocity of the CoM passes the usual value of the vertical velocity at touch-down it means the robot encounters a step down in the ground. Therefore, the leg actuator extends the leg towards the ground. Because of the existence of the motor inertia and maximum torque, the toe reaches the ground with some delay. Meantime, the leg angle is adjusted based on the current leg length

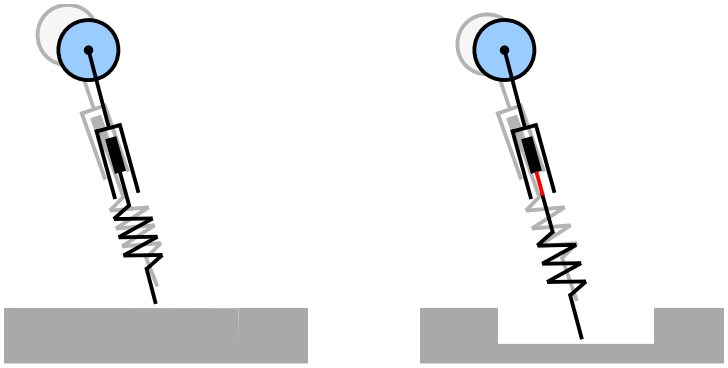

Figure 3.6: **Left:** The leg actuator does not work on even ground (no leg extension, only leg angle adjustment during the flight phase) **Right:** The leg actuator extends the leg, the leg angle is adjusted concurrently based on the current leg length.

to have symmetric gait in stance phase whenever it hits the ground.

3.3 Results

The CoM trajectory of the robot controlled with the policy described in section 3.2 is shown in Figure 3.7. When the vertical velocity of the CoM becomes greater than the vertical velocities at touch-down in previous strides, the leg actuator starts extending the leg towards the ground. At each moment, based on the new leg length and new vertical velocity the required touch-down angle is calculated from the look-up table. Figure 3.8 shows the leg force profiles for three cases. As can be seen in the figure, the increase in the peak force with the proposed control policy is only 11% more than the undisturbed case. This increase is due to the small increase in the vertical velocity of the CoM while the motor tries to hit the ground. The increase of the peak force due to the Ernst et. al. [23] method is about 33% more than the undisturbed case.

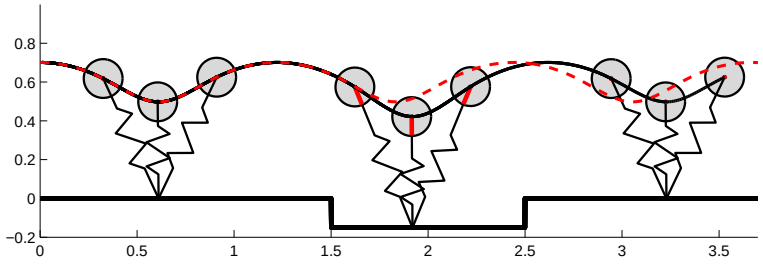

Figure 3.7: The actuated SLIP model rapidly extends the leg and adjusts the leg angle concurrently. The red line on the leg at the drop gait is the increased leg length.

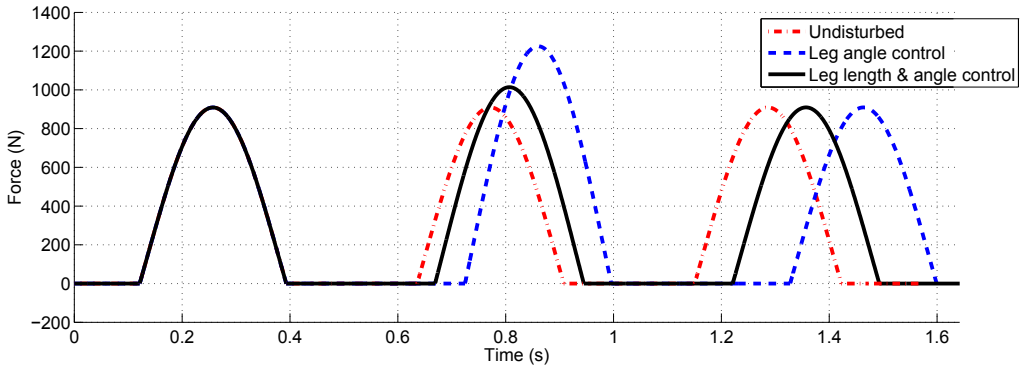

Figure 3.8: Leg force profiles show the peak force increases only 11% if the leg is rapidly extended. This increase is due to the physical limitations of the motor like motor inertia. Without leg extension, increase in leg force would be 33%.

3.4 Conclusion

In this paper we proposed a bio-inspired control strategy for the flight phase that leads to steady state running but more importantly keeps the leg force nearly constant in the presence of disturbances. The proposed control policy comes from the fact that if the leg length extends while the leg angle is being adjusted appropriately (like animals do), the peak force in the leg does not increase too much. It means the leg extension partially compensates for the drop and the leg angle is updated to generate the symmetric path. It should be noted that the small increase in the leg force in our simulation is due to the physical limitations of the motors that prevent them to act instantaneously.

Chapter 4 – Optimum passive elements for jumping: throwing the body mass

The passive dynamics of actuators may impose serious limitations to the performance of a system. Existence of inertia for example makes it impossible for the actuators to react immediately. A throwing mechanism (with electric motors) is composed of two inertias (object and motor) that decreases the performance of the system and can not be overcome with software control. But, we can use other elements (like a spring) to make the motor inertia a benefit to improve the performance of the system. Moreover, when the object is directly connected to the motor, the maximum velocity that the object can achieve is limited to the maximum velocity that can be provided by the motor. Here, we will extract mathematical formula that gives us the required optimum value for stiffness and/or damping of the system to give us the optimal performance given physical limitations.

4.1 Introduction

Physical interaction tasks like catching and throwing (i.e jumping and landing) are done by animals much better than robots. Although rigid robots are very good at some tasks like accurate positioning of objects, they perform poorly in accomplish-

ing physical interaction tasks. We think that most of the amazing performance of animals is due to the physical characteristics of their mechanical systems and their synchronicity of their control policy.

Throwing an object directly by a rigid robot which is driven by electric motor is limited to the maximum velocity that the motor can provide. In this case, to reach the maximum possible velocity, the robot applies the maximum force (or torque) to the system until either the motor reaches the limit of its range of motion or the object reaches the maximum velocity of the motor. By using the characteristics of springs and dampers, the performance of the system can be improved significantly.

The idea of using spring for throwing a mass is to store energy in the spring in the beginning of the process to help the motor push the object faster while the motor is at its maximum velocity. In this process, the inertia of the motor helps the system to accelerate the object even more. Since the idea is to transfer as much energy as possible to the object, the existence of damper which dissipates energy seems destructive. However, considering the other mechanical limitations like maximum motor range of motion or maximum allowable spring compression, the existence of damping can become beneficial.

Regardless of the software and controller, there are some physical limitations that impose serious limits. The motor inertia which is amplified through the gearbox or the maximum distance that the motor can travel are among the physical limitations that the software can not overcome. In the other words, no matter which controller is used, the motor can not travel further than its maximum limit or the motor can not respond instantly and generate the desired velocity. In this paper we use an

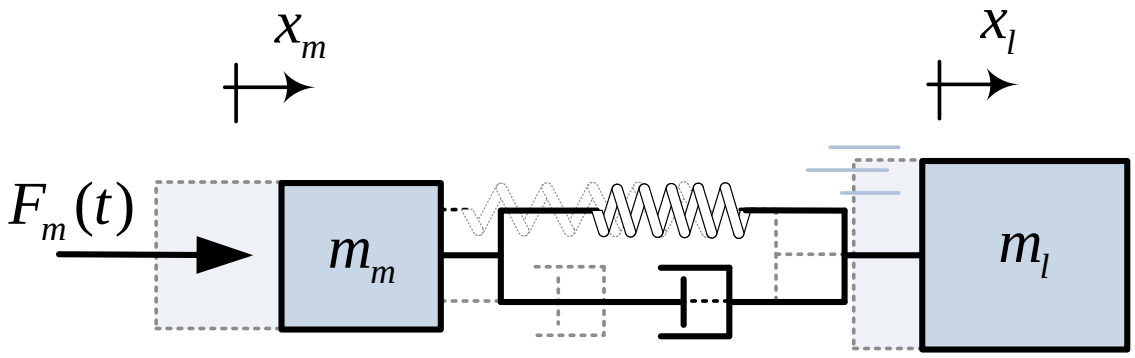

Figure 4.1: The system we investigate in this paper is entirely linear and includes damping, elasticity, motor inertia (represented as an equivalent mass), motor force limits and motor maximum velocity as well as maximum spring compression length.

schema for throwing an object and present formulations to calculate the optimal values for the parameters of the new system (elasticity and damping) to have an optimal physical performance. In the mathematical framework of our mechanical system we consider inertia, torque limit and velocity limit for the electric motor in series with a spring-damper system (which has also compression limit) as shown in figure 4.1.

4.2 Background

The motivation of this paper is to investigate the effect of elasticity and damping on initializing the process of running for a legged robot from its rest position using electric motors. Other researchers have used the subject of throwing for robot's arms [36][37], hopping [38] or as a new method for transportation of objects[39][40].

The mechanism of running and walking in animals can be best presented by

spring-mass model [2][41]. Although roboticists who have built machines to mimic spring-like behavior [42][28][43] acknowledged that elasticity provides robustness, but their studies focused on energy storage and efficiency. Little attention is given to how these elements contribute to general force control and manipulation with the environment. Recently [38] investigated the effect of compliant actuator on the energy efficiency of a hopping robot. They concluded that series elastic elements help the robot to achieve higher hopping hight.

Early investigations into force control found that series compliance in an actuator can increase stability, and in some cases is required for stable operation [44]. Researchers at the Massachusetts Institute of Technology (MIT) Leg Laboratory explored these ideas and created the Series Elastic Actuator (SEA). The MIT-SEA is designed specifically to include an elastic element as a force sensor and low impedance coupling between the drive system and the load to improve force control. It has been shown that this configuration provides filtering to handle shock loads and higher bandwidth force control [45].

Hurst et al. [46] proposed an extension to MIT-SEA. They investigated the effect of damping and concluded that the added damping provides higher bandwidth than a purely series-elastic element. But, initial observed force by the drive system at impact is greater than a system that is only composed of an elastic element.

Haddadin et al. [47] showed that it is possible to derive suitable stiffness for an elastic joint and it is capable of at least reaching the maximum velocity of the rigid joint.

Braun et al. [48] proposed an optimal stiffness profiles for a variable stiffness

system. They chose throwing a ball to demonstrate their method. Garabini et al. [49] also investigated the optimality principles in stiffness control. They imposed a fixed terminal time in their optimization program to maximize the velocity of the actuator link.

Throwing an object has been considered a means in transporting objects[40] [39]. Frank et. al. in [40], used a rigid rotary system to throw the objects. A rotary electric motor is connected to the rigid arm with a specific length (which is determined based on the desired final velocity) and the mass is located at the end of the arm. To increase the final velocity of the thrown objects, the length of the arm should be increased which increases the inertia of the system quadratically ($I = I_0 + m \cdot d^2$).

In this paper we show quantitatively how the spring and damping affect the behavior of the throwing mechanism. Moreover, we will present mathematical formulations to relate the various parameters of the actuator. It will be shown that for various physical limitations (such as motor/spring stroke) there is an optimum value for stiffness and damping that gives us the greatest final velocity.

4.3 Problem definition

To investigate the effect of elasticity and damping on the performance of throwing, the system in Fig. 4.2 is considered. In the mathematical model of the system, in addition to the elements k and B, we include motor force limits, motor inertia and motor velocity limit as well as maximum spring compression length. The motor torque and rotational inertia are modeled as a linear mass with applied force (similar

to a ballscrew). The following symbols describe our mathematical model:

k	Spring constant	$N \cdot m$
B	Damping constant	$\frac{N \cdot s}{m}$
m_m	Motor/transmission mass	kg
m_L	Load mass	kg
F_m	Motor force	N
F_{limit}	Motor force limit	N
F_d	Force caused by the dynamic elements	N
v_{max}	Motor maximum velocity	$\frac{m}{s}$

We assume that the actuator can not sustain tension (like jumping) therefore the final velocity of the object is the velocity that it has at the first loss of contact (unlike the case for pogo sticks that to reach the maximum velocity, it losses the contact several times). Our goal in this paper is to show how to calculate the optimum values for stiffness and damping to be added to the passive dynamics of the system to improve the performance the most (means maximizes the final velocity of the object).

4.4 Mathematical formulation

To model the effects of the passive dynamics of an actuator to the performance of our system, the system shown in Fig. 4.2 is considered. We want to know how to choose the values of elasticity and damping (k and B) to have the most efficient throwing

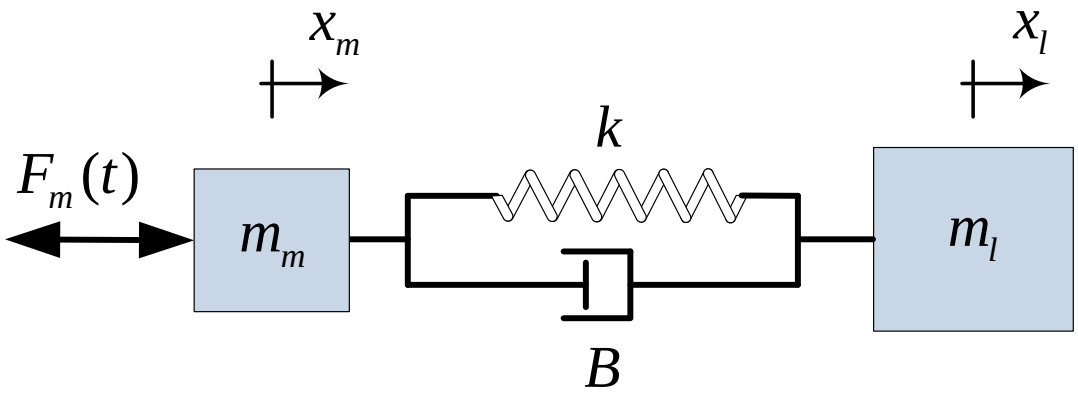

Figure 4.2: System schematic. The motor inertia is represented as a linear mass (m_m) and the load mass is represented as (m_l). This is analogous to an electric motor attached to a ballscrew transmission where the rotational inertia is much greater than the mass of the transmission itself.

system given our physical limitations like stroke limit. Moreover, the system shown in Fig. 4.2 is similar to the mechanism of legged robots [42] [28].

We define the performance of the system as the largest possible v that the object can reach without breaking the contact to the system given the physical limitations. In our model, the spring is linear and the damper is a viscous damper, therefore the dynamical behavior of the system is linear. The differential equations that describe the motion of the system are:

$$[m]\begin{Bmatrix}\ddot{x}_l\\ \ddot{x}_m\end{Bmatrix}+[B]\begin{Bmatrix}\dot{x}_l\\ \dot{x}_m\end{Bmatrix}+[k]\begin{Bmatrix}x_l\\ x_m\end{Bmatrix}=\begin{Bmatrix}0\\ F_m\left(t\right)\end{Bmatrix} \tag{4.1}$$

where

$$[B] = \begin{bmatrix} B & -B \\ -B & B \end{bmatrix} \tag{4.2}$$

$$[k] = \begin{bmatrix} k & -k \\ -k & k \end{bmatrix} \tag{4.3}$$

$$[m] = \begin{bmatrix} m_l & 0 \\ 0 & m_m \end{bmatrix} \tag{4.4}$$

Here, the $[B]$, $[k]$ and $[m]$ are respectively damping, stiffness and mass matrices. As the system of differential equations (eq. 4.1) is coupled, it can not be solved in this form. To solve the system, we decoupled (4.1) into two independent single degree of freedom (SDOF) systems using the system's mode shapes [50]. Therefore, the initial degrees of freedom can be mapped by the mode shape vectors of the system to a new set of degrees of freedom as follows:

$$\begin{Bmatrix} x_l \\ x_m \end{Bmatrix} = \{\phi\}_1 z_1(t) + \{\phi\}_2 z_2(t) \tag{4.5}$$

$$\{\phi\}_1 = \begin{Bmatrix} 1 \\ 1 \end{Bmatrix} \qquad \{\phi\}_2 = \begin{Bmatrix} 1 \\ -\mu \end{Bmatrix} \tag{4.6}$$

Which here, $\{\phi\}_1$ and $\{\phi\}_2$ are the mode shapes of the system. Because of the orthogonality characteristic of the mode shapes respect to mass and stiffness matrices [50], the original differential equation (eq. 4.1) can be split to the following

independent equations.

$$(m_l + m_m)\,\ddot{z}_1(t) = F_m(t) \tag{4.7}$$

$$m_e\ddot{z}_2(t) + B_e\dot{z}_2(t) + k_e z_2(t) = -\mu F_m(t) \tag{4.8}$$

where the equivalent parameters used here, are defined as follows:

$$m_e = m_l(1+\mu) \tag{4.9}$$

$$B_e = B(1+\mu)^2 \tag{4.10}$$

$$k_e = k(1+\mu)^2 \tag{4.11}$$

$$\mu = \frac{m_l}{m_m}. \tag{4.12}$$

The two new models demonstrated in Fig. 4.3 are the two new independent degrees of freedom. The left figure represents the rigid body motion of the system (z_1) and describes how the masses move together. On the other hand, the right figure describes the oscillation of the masses relative to each other (z_2). The whole response of the system is composed of a linear combination of these two independent motions as described by eq. 4.5.

Since we are looking for the case that gives us the largest final velocity, the motor should apply its maximum force from the beginning. It should be noted that here, like the case of jumping, the system of spring-damper can not sustain tension. Equation 4.7 can be easily solved by integrating that equation two times respect to

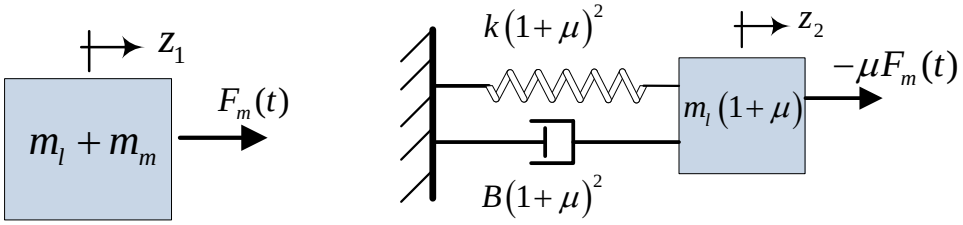

Figure 4.3: The original system in Fig. 4.2 can be broken into two separate single degree of freedom systems.

time (t). On the other side, equation 4.8 is the well-known SDOF oscillation system [50]. The closed form solutions of the above equations are as follows:

$$z_1(t) = \frac{F_{max}}{2(m_l + m_m)}\left(t^2\right) \tag{4.13}$$

$$z_2(t) = -\frac{\mu F_{max}}{(1+\mu)k_e}\left(1 - A(t)\right) \tag{4.14}$$

$$A(t) = e^{-\zeta w_e t}\left(\frac{\zeta}{\sqrt{1-\zeta^2}}\sin(w_d t) + \cos(w_d t)\right) \tag{4.15}$$

Other parameters used in the above equations are:

$$w_e = \frac{k(1+\mu)}{m_l} \tag{4.16}$$

$$\zeta = \frac{B_e}{2m_e w_e} \tag{4.17}$$

$$w_d = w_e\sqrt{1-\zeta^2} \tag{4.18}$$

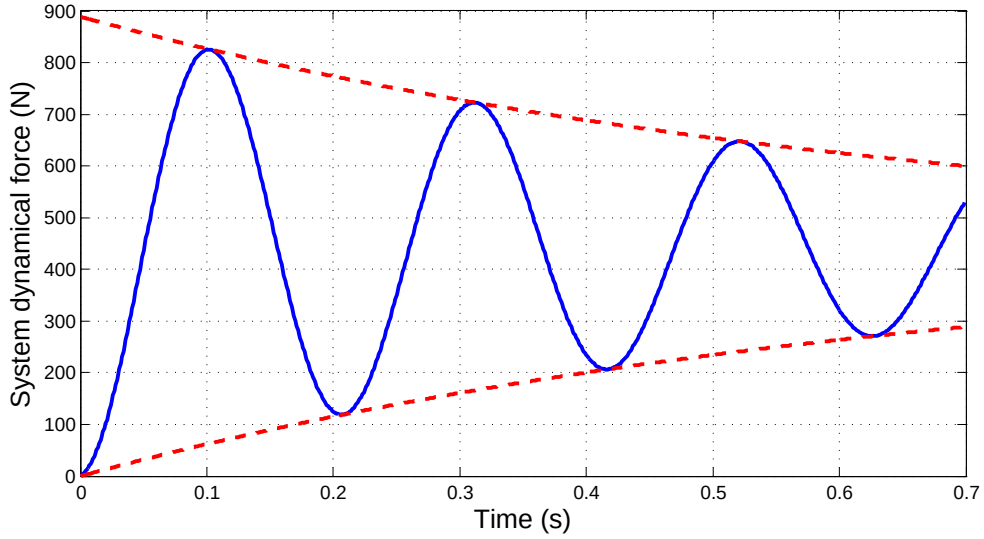

Figure 4.4: Variation of the dynamical force of the spring-damper system to the object respect to time.

Here, w_e, ζ and w_d are respectively natural frequency, damping ratio and damped frequency of the equivalent system. The relative movement of the masses respect to each other (z_2 and $\dot{z}_2$) determines the contact between the object and the system. As the eq. 4.14 is like a constant force applying on a single degree of freedom system, the reaction force of the support never passes the zero line in the existence of damping. When there is no damping in the system, the dynamical force touches the zero line, but still never crosses that line. Fig. 4.4 shows how dynamical force of the system ($B \cdot \dot{z}_2 + k \cdot z_2$) varies respect to time. It can be concluded that as long as the motor applies the maximum force to the system, the object will not leave the system and consequently it means that the object is accelerated until some hard stops happen.

The first hard stop that should be controlled is the spring length limit. To control the adequacy of the stiffness and/or damping of the system to satisfy the spring limit

length equation 4.14 is used. The required spring deflection is determined by the maximum possible value for the oscillation degree of freedom (z_2) which is represented in equation 4.8. Therefore, the relation between the physical characteristics of the system and the maximum possible spring deflection can be obtained as follows:

$$l_{spring} = \frac{\mu F_{max}}{(1+\mu)^2 k}\left(1 + e^{-\zeta\pi}\right) \tag{4.19}$$

It is the first and the simplest equation to calculate the required stiffness and/or damping of the system. The largest value for the required stiffness is when the damping is equal to zero. Also it can be understood that damping has not significant effect on limiting the spring compression.

The relative movement of the two masses shows if the object leaves the system or not. If the dynamic force applied by the spring and damper becomes zero, it means the object is on the onset of the separation. Based on the eq. 4.14, the relative equation of the masses is like a single degree of freedom under a constant force. The variation of this function is shown in Fig. 4.4

To satisfy other physical limitations of the actuator, two scenarios may happen. In the first scenario, the motor reaches its maximum length before reaching its maximum velocity and the second one is that motor reaches its maximum velocity before reaching its maximum length. For the first scenario, the system follows a single rule, but for the second one, the dynamics equation of the system alters when the motor reaches its maximum velocity (means the motor does not apply force when it is at its maximum velocity).

The velocities of the object and the motor can be obtained as follows:

$$\dot{x}_l(t) = \frac{F_{max}}{m_l + m_m}\left(t - \frac{1}{w_d}e^{-\zeta w_e t}\sin(w_d t)\right) \tag{4.20}$$

$$\dot{x}_m(t) = \frac{F_{max}}{m_l + m_m}\left(t + \frac{\mu}{w_d}e^{-\zeta w_e t}\sin(w_d t)\right) \tag{4.21}$$

The first term in the parenthesis above is common for both load velocity and motor velocity which shows the rigid body motion of the system. But, the second term shows the relative motion between the object and the motor. In the ideal situation where there was no motor limitations, we just needed to find a stiffness correspond to maximizing the second term. In the real situation that we do have physical limitations like motor length limit and motor velocity limit, the first term (means the time that the motor drives the system) also influences the results and makes the analysis of the system far more complicated. To consider the motor length limit, we need the position of the motor at each instant. The positions of the load and the motor are:

$$x_l(t) = \frac{F_{max}}{m_l + m_m}\left(0.5t^2 - \frac{1}{w_e^2}(1 - A(t))\right) \tag{4.22}$$

$$x_m(t) = \frac{F_{max}}{m_l + m_m}\left(0.5t^2 + \frac{\mu}{w_e^2}(1 - A(t))\right) \tag{4.23}$$

$$A(t) = e^{-\zeta w_e t}\left(\frac{\zeta}{\sqrt{1-\zeta^2}}\sin(w_d t) + \cos(w_d t)\right) \tag{4.24}$$

Since the motor can not travel more than its maximum length, the second equa-

tion above should be less than or equal to the maximum motor length. This equation relates the motor travel length limit to the physical characteristics of the system.

$$l_{motor} = \frac{F_{max}}{m_l + m_m} \left(0.5 t_f^2 + \frac{\mu}{w_e^2} \left(1 - A\left(t_f\right) \right) \right) \tag{4.25}$$

Which $A\left(t_f\right)$ is given in eq. 4.24. This equation should be solved respect to the time (t_f) which shows the time of the process. After that, everything can be obtained by the equations 4.20 to 4.23.

4.5 Simulation

Because of the complicated form of the mathematical formulas, understanding the role of each parameter on the behavior of the system is not easy. In this section, based on the closed form solutions in the previous section, we present simulations to show the effect of the physical parameters on the behavior of the system by graphs. To accomplish the simulations, following characteristics are assumed for the system.

Parameter	**Description**	**Value**
m_m	Motor/transmission mass	$5kg$
m_l	Load mass	$10kg$
l_{spring}	Spring maximum length	$1m$
l_{motor}	Motor maximum length	$1m$
F_{max}	Motor maximum force	$1000N$
v_{max}	Motor maximum velocity	$5\frac{m}{s}$

The two scenarios mentioned before are investigated here in simulation. In the first scenario, we assume that the motor can reach any velocity until the maximum length of the motor. For the second scenario, in addition to the motor length limit, the motor can not pass a predefined velocity.

4.5.1 Motor length determines the final velocity

In this scenario, we assume that the motor length limits the final velocity. Therefore, we can assume there is no limit on the motor velocity. It makes the equations simpler and gives us good information about the dynamics of the system. Figure 4.5 shows how damping and spring stiffness affect the maximum load velocity. The object gets its maximum velocity at the first peak. Also the largest value for the velocity is obtained when there is no damping in the system. The straight dashed line shows the velocity when the motor was directly connected to the object and it is accelerated until the motor hard stop occurs. Interesting note here is that, when for some reasons we could not provide the most optimum stiffness (like for example having a very small

limit for spring length), there are some other choices far stiffer than that. If we have a tight spring limit concern we should no use any damper in the system, otherwise the behavior of the system will not be improved significantly.

To generate the response graphs in Fig. 4.5, the motor should at least provide the velocities shown in Fig. 4.6. In this figure, the maximum motor velocity for different spring stiffnesses is shown. As can be seen in both figures 4.5 and 4.6, to have the highest thrown velocity (which is about 13 m/s in this simulation) the motor should just have the maximum velocity about 8 m/s (means about 50 percent less). When the motor can not provide that velocity, the dynamic equation of the system changes and the behavior of the system will not be the same as was shown earlier. Interesting note in these figures is that, in about the same stiffness that the object gets its maximum velocity, the motor needs the smallest velocity.

4.5.2 Motor velocity limit determines the final velocity

The velocity limit on the motor alters the dynamics of the system. When the motor reaches its maximum velocity, it can no longer apply force to the system and the combined system travels with a constant velocity (but with relative motion respect to each other). This change in the dynamics of the system, changes the shape of the graphs in Fig. 4.5. The new response of the system is shown in Fig. 4.7. Two dashed straight lines in this graph show the velocities correspond to the motor length limit (top one) and motor velocity limit (bottom one). Adding elasticity to the system amplifies the maximum velocity of the object to about twice the value that it could

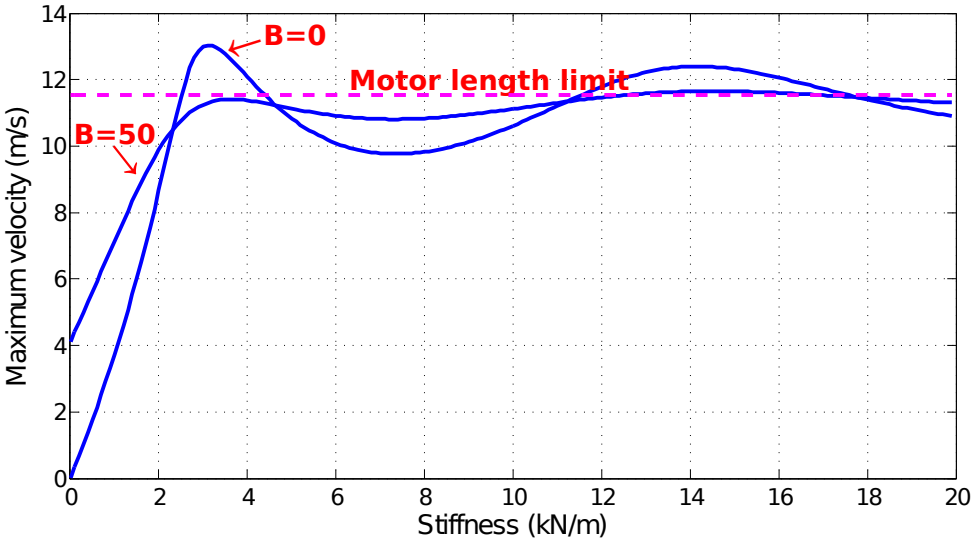

Figure 4.5: The effect of spring stiffness on the maximum velocity of the object for the case of undamped ($B = 0$) and with damping equal to $B = 50$. The dashed straight line shows the velocity of the object when it is rigidly connected to the motor and no motor velocity limit is assumed.

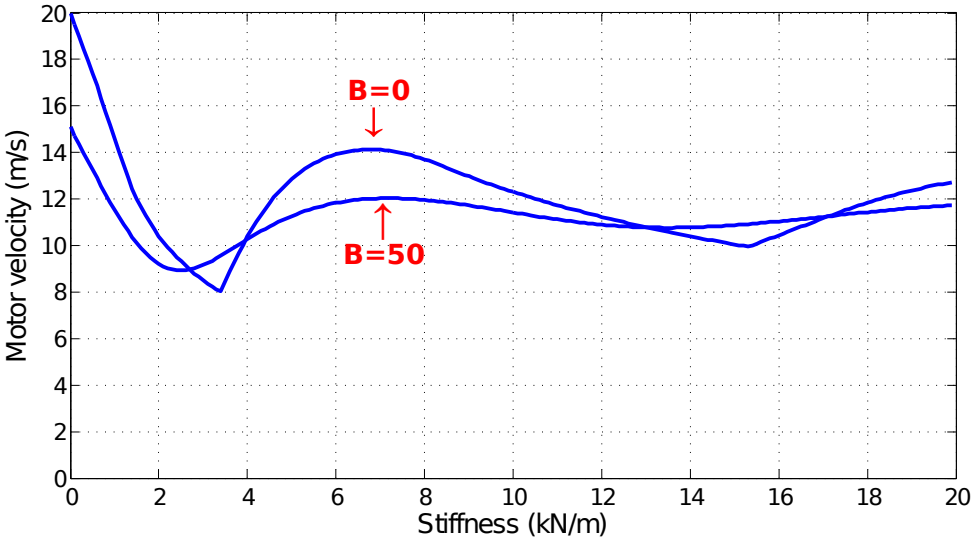

Figure 4.6: The variations of maximum motor velocity respect to the stiffness of the spring in the case of undamped system ($B = 0$) and with damping equal to $B = 50$.

have without the spring. Therefore, for the systems with low motor velocity limit, using appropriate spring and damper can improve the performance of the actuator significantly. The stiffness value corresponded to the highest velocity in Fig. 4.5 is still among the best choices for the stiffness. Moreover, the range of the spring stiffnesses that gives us the highest velocity was increased. Also it can be understood from the graph that damping has not significant effect on the response of the system for stiffnesses more than a certain value.

Another parameter that highly influences the final velocity of the object is the maximum force that can be provided by the motor. Figure 4.8 shows how the motor maximum force affects the final velocity of the thrown object. Based on the closed form solutions, the increase in velocity is linear.

For the case that we have velocity limit for the motor, the maximum motor force

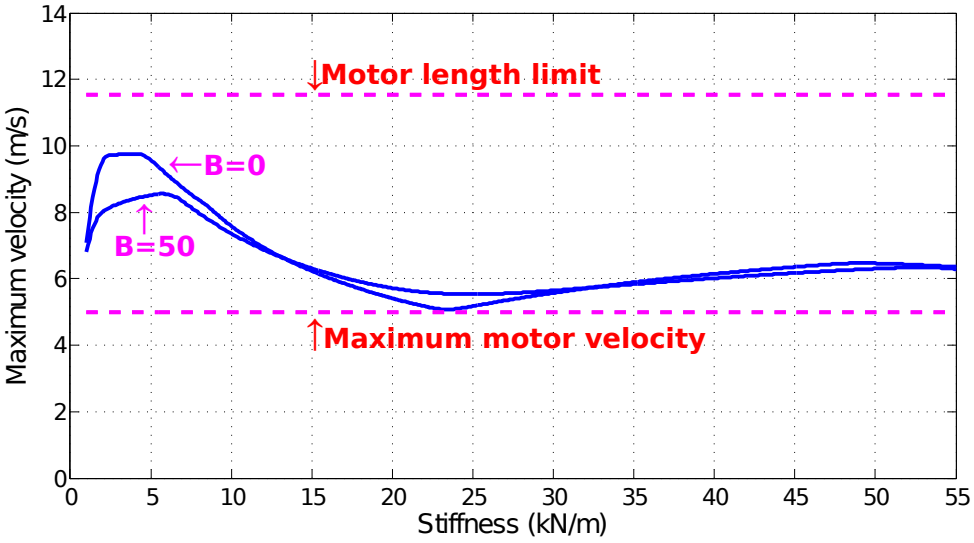

Figure 4.7: Motor maximum velocity changes the shape of the response, but the optimum stiffness value remains optimum.

can not increase the final velocity beyond a certain value (Fig. 4.9). In Fig. 4.9 the responses of the system for three different motor forces are shown. When we have motor velocity limit, increasing the motor force can be not useful. Also, no matter what stiffness is chosen, the maximum achievable velocity will be constant. In these cases, if we need higher velocity, we have to increase the motor velocity limit.

4.6 Conclusions

In this paper, we extracted mathematical formulas for calculating the optimum stiffness and/or damping to be added to the passive dynamics of a system to enhance the performance of a throwing mechanism. By the use of the eigenvectors of the system, we simplified the equations to two independent single degree of freedom sys-

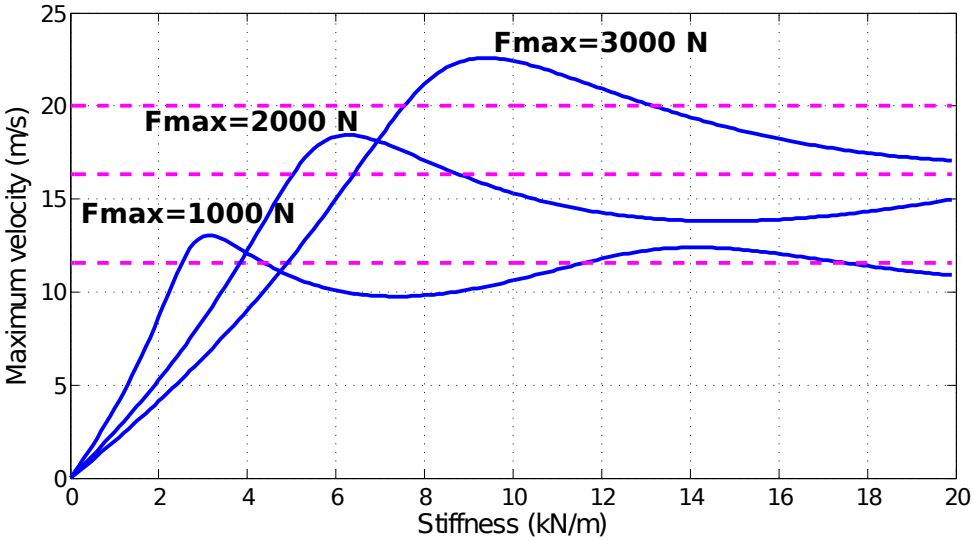

Figure 4.8: The effect of the maximum motor force on the response of the system. Here, the system has no damping. As the maximum motor force increases the optimum required stiffness of the spring increases as well.

tems. Based on the extracted formulas and interpretations of the results from the simulation we can conclude that:

1. Adding elasticity and/or damping to the actuator if chosen accurately, improves the performance of the system. However, if these values are not used accurately, the outcome can even decrease the performance.

2. For each system, if we do not have motor velocity limit, there is a stiffness value that improves the performance of the system the most. Also, there are other stiffer values for the spring that improves the final velocity but not the same as the initial one.

3. The mechanical limitations like actuator range of motion directly affect the

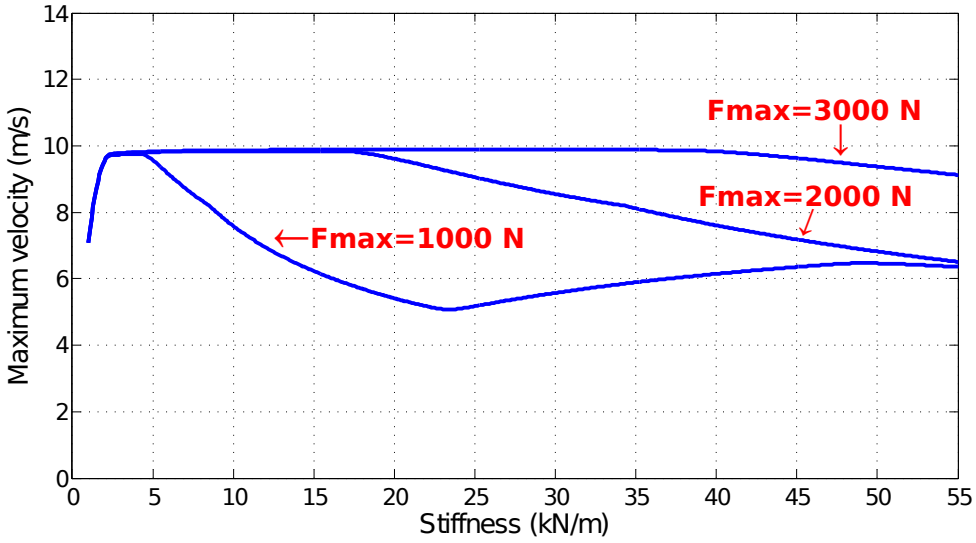

Figure 4.9: The effect of the maximum motor force on the response of the system while we have motor velocity limit. The graphs are for non-damped cases. The highest velocity remains unchanged for different motor forces.

required stiffness of the spring.

4. Motor velocity is minimized for the stiffness that gives the object the largest velocity.

5. For the cases that we have low maximum motor velocity, adding spring-damper system can improve the performance of the system.

6. When the motor has low maximum motor velocity, increasing the motor force to improve the final velocity of the object, is not helpful. In this case, it is recommended to use gearbox to increase the motor velocity instead of the motor force.

We defined relationships between series stiffness, series damping, drive system inertia, drive system torque limits, the drive velocity limit and the maximum velocity that the object can achieve using the mathematical model shown in Fig. 4.2. The linear spring was chosen because of its simplicity and its similarity to the SLIP (Spring-Load Inverted Pendulum) model used in legged locomotion. For future work, we plan to investigate the effect of the nonlinearity of the spring on the behavior of the system.

Chapter 5 – Conclusion

We have proposed two types of flight phase control strategies for spring-mass running robots and derived mathematical framework for the design of the passive elements of these robots for the initiation of running. The control policies are all during flight phase and the system is purely passive in stance phase following the passive dynamics behavior of the system. In our control policies, we targeted two important goals for real robots: damage avoidance and energy efficiency, to have a safe and efficient running.

In chapter 2 we considered the leg angle as the only control parameter during the flight phase to control spring-mass running robots. In the proposed control policies we investigated in this chapter, the leg peak force, axial impulse and leg actuator work during stance phase were considered as the objective functions to be regulated by adjusting the leg angle during the flight phase. We found out that by regulating any of these three objective functions, both goals of damage avoidance and energy efficiency would be fulfilled at once. Results showed that implementing these policies in real robots are as easy as implementing a constant angular acceleration for the leg retraction during the flight phase. Furthermore, we proposed a new graph that depicts the behavior of the flight phase control policies in the presence of ground level changes. By the help of this graph, the limitations of the flight phase control policies (like the maximum drop height that can be rejected to have a successful

stance phase) can be found. The general conclusions for this chapter are:

- Considering damage avoidance and/or energy efficiency as the primary goals during running is crucial for economically designed running robots and leads to the same behavior that we observe from animals' running.
- When regulating any of the three proposed objective functions (peak force, axial impulse or leg actuator work) during running, both goals of damage avoidance and energy efficiency are fulfilled at once.
- Implementing a constant leg angular acceleration is enough to regulate either of the proposed objective functions (leg peak force, axial impulse or leg actuator work).
- The control policies are feed-forward and there is no need for any external sensing.

In chapter 3 we used both leg length and leg angle as the control parameters for the flight phase. In this chapter the main focus was retaining steady state running in the presence of hidden disturbances and minimizing the leg peak force that the robot would have during the passive stance phase. The results showed that using the leg length can significantly reduce the leg peak force while retaining the equilibrium gait in running.

In chapter 4 we derived mathematical formulas for the design of the passive elements in spring-mass running robots for initiating running. The problem of jumping is mathematically equal to throwing an object, therefore we focused on the problem of throwing a load mass by motor with rotor inertia and maximum motor torque

capacity. We showed that using appropriate spring and damper can enhance the performance of the system. One interesting result is that even though it is thought that damper would reduce the performance of throwing problem, appropriate damping can even enhance the performance of the system and make the robot jump even higher. The general conclusions for this chapter are:

- Adding elasticity and/or damping to the actuator if chosen accurately, improves the performance of the system. However, if these values are not used accurately, the outcome can even decrease the performance.

- Motor velocity is minimized for the stiffness that gives the object the largest velocity.

- Increasing the motor force to improve the final velocity of the object is not always helpful. There should be a trade-off between the motor maximum velocity and motor maximum torque. When the motor has low maximum motor velocity, it is recommended to use gearbox to increase the motor velocity and accept the decrease in maximum motor force.

By the results of this work, roboticists can optimally design the passive elements of spring-mass running robots to achieve the maximum possible speed. When the running started, the control strategies allow the robot to continue the running primarily based on the passive dynamics of the system and hence it will be very efficient. The focus of the control policies is on the peak force generated in the leg during the stance phase to avoid leg damage and have a safe running in uneven terrain. Surprisingly, the implementation of the proposed control policies are very easy and requires

minimal sensing.

Bibliography

[1] R. Blickhan, "The spring mass model for running and hopping," *Journal of Biomechanics*, vol. 22, no. 11-12, pp. 1217–1227, 1989.

[2] A. Seyfarth, H. Geyer, M. Guenther, and R. Blickhan, "A movement criterion for running," *Journal of Biomechanics*, vol. 35, pp. 649–655, 2002.

[3] D. Koepl and J. Hurst, "Force control for planar spring-mass running," in *Intelligent Robots and Systems (IROS), 2011 IEEE/RSJ International Conference on*, (San Francisco, USA), 2011.

[4] U. Saranli, M. Buehler, and D. E. Koditschek, "RHex: A simple and highly mobile hexapod robot," *International Journal of Robotics Research*, vol. 20, pp. 616–631, 2001.

[5] A. Altendorfer, N. Moore, H. Komsuoglu, M. Buehler, H. B. Brown Jr., D. McMordie, U. Saranli, R. J. Full, and D. E. Koditschek, "Rhex: A biologically inspired hexapod runner," *Autonomous Robots*, vol. 11, no. 3, pp. 207–213, 2001.

[6] M. Raibert, K. Blankespoor, G. Nelson, R. Playter, and t. B. Team, "Bigdog, the rough-terrain quadruped robot," in *World Congress of the International Federation of Automatic Control*, (Seoul, Korea), 2008.

[7] J. W. Grizzle, J. Hurst, B. Morris, H.-W. Park, and K. Sreenath, "MABEL, a new robotic bipedal walker and runner," in *Conference on American Control Conference*, (St. Louis, USA), 2009.

[8] J. Grimes and J. Hurst, "The design of atrias 1.0 a unique monopod, hopping robot," in *International Conference on Climbing and Walking Robots*, (Baltimore, USA), 2012.

[9] A. D. Kuo, "Choosing your steps carefully," *IEEE Robotics & Automation Magazine*, vol. 14, pp. 18–29, 2007.

[10] Y. Blum, H. R. Vejdani, A. Birn-Jeffery, C. Hubicki, J. Hurst, and M. A. Daley, "Trade-off between disturbance rejection and injury avoidance in running guinea fowl," *PloS One*, vol. submitted, 2013.

[11] H. Geyer, A. Seyfarth, and R. Blickhan, "Compliant leg behaviour explains basic dynamics of walking and running," *Proceedings of the Royal Society B*, vol. 273, pp. 2861–2867, 2006.

[12] A. Seyfarth, H. Geyer, and H. Herr, "Swing-leg retraction: A simple control model for stable running," *Journal of Experimental Biology*, vol. 206, pp. 2547–2555., 2003.

[13] Y. Blum, S. W. Lipfert, J. Rummel, and A. Seyfarth, "Swing leg control in human running," *Bioinspiration & Biomimetics*, vol. 5, p. 026006, 2010.

[14] M. Ernst, H. Geyer, and R. Blickhan, "Extension and customization of self-stability control in compliant legged systems," *Bioinspiration & Biomimetics*, vol. 7, no. 4, p. 046002, 2012.

[15] C. T. Moritz and C. T. Farley, "Passive dynamics change leg mechanics for an unexpected surface during human hopping," *Journal of Applied Physiology*, vol. 97, pp. 1313–1322, 2004.

[16] M. A. Daley, A. Voloshina, and A. A. Biewener, "The role of intrinsic muscle mechanics in the neuromuscular control of stable running in the guinea fowl," *Journal of Physiology*, vol. 587, p. 26932707, 2009.

[17] M. A. Daley and A. A. Biewener, "Leg muscles that mediate stability: mechanics and control of two distal extensor muscles during obstacle negotiation in the guinea fowl," *Philosophical Transactions of the Royal Society B*, vol. 366, pp. 1580–1591, 2011.

[18] A. Birn-Jeffery and M. A. Daley, "Birds achieve high robustness in uneven terrain through active control of landing conditions," *Journal of Experimental Biology*, vol. 215, pp. 2117–2127, 2012.

[19] M. A. Daley and A. A. Biewener, "Running over rough terrain reveals limb control for intrinsic stability," *Proceedings of the National Academy of Sciences of the USA*, vol. 103, pp. 15681–15686, 2006.

[20] H. M. Herr and T. A. McMahon, "A galloping horse model," *International Journal of Robotics Research*, vol. 20, pp. 26–37, 2001.

[21] M. A. Daley and J. R. Usherwood, "Two explanations for the compliant running paradox: Reduced work of bouncing viscera and increased stability in uneven terrain," *Biology Letters*, vol. 6, pp. 418–421, 2010.

[22] Y. Blum, A. Birn-Jeffery, M. A. Daley, and A. Seyfarth, "Does a crouched leg posture enhance running stability and robustness?," *Journal of Theoretical Biology*, vol. 281, pp. 97–106, 2011.

[23] M. Ernst, H. Geyer, and R. Blickhan, "Spring-legged locomotion on uneven ground: a control approach to keep the running speed constant," in *International Conference on Climbing and Walking Robots*, (Istanbul, Turkey), 2009.

[24] J. Karssen, M. Haberland, M. Wisse, and S. Kim, "The optimal swing-leg retraction rate for running," in *Robotics and Automation (ICRA), 2011 IEEE International Conference on*, pp. 4000 –4006, may 2011.

[25] T. A. McMahon and G. C. Cheng, "The mechanics of running: How does stiffness couple with speed?," *Journal of Biomechanics*, vol. 23, pp. 65–78, 1990.

[26] R. J. Full and D. E. Koditschek, "Templates and anchors: Neuromechanical hypotheses of legged locomotion on land," *Journal of Experimental Biology*, vol. 202, pp. 3325–3332., 1999.

[27] A. Seyfarth and H. Geyer, "Natural control of spring-like running: optimized self-stabilization," in *International Conference on Climbing and Walking Robots*, (London, UK), 2002.

[28] M. H. Raibert, *Legged Robots That Balance*. Cambridge: The MIT Press, 1986.

[29] A. Altendorfer, D. E. Koditschek, and P. Holmes, "Stability analysis of a clock-driven rigid-body slip model for rhex," *The International Journal of Robotics Research*, vol. 23, no. 10-11, pp. 1001–1012, 2004.

[30] J. Schmitt and J. Clark, "Modeling posture-dependent leg actuation in sagittal plane locomotion," *Bioinspiration & Biomimetics*, vol. 4, pp. 17–33, 2009.

[31] B. Miller, J. Schmitt, and J. E. Clark, "Quantifying disturbance rejection of slip-like running systems," *The International Journal of Robotics Research*, vol. 31, no. 5, p. 573587, 2012.

[32] B. Andrews, B. Miller, J. Schmitt, and J. E. Clark, "Running over unknown rough terrain with a one-legged planar robot," *Bioinspiration & Biomimetics*, vol. 6, no. 2, p. 026009, 2011.

[33] F. Parietti and H. Geyer, "Reactive balance control in walking based on a bipedal linear inverted pendulum model," in *Robotics and Automation (ICRA), 2011 IEEE International Conference on*, pp. 5442 –5447, may 2011.

[34] R. M. Ghigliazza, R. Altendorfer, P. Holmes, and D. Koditschek, "A simply stabilized running model," *SIAM Review*, vol. 47, pp. 519–549, 2005.

[35] M. A. Daley, J. R. Usherwood, G. Felix, and A. A. Biewener, "Running over rough terrain: guinea fowl maintain dynamic stability despite a large unexpected change in substrate height," *The Journal of Experimental Biology*, vol. 209, pp. 171–187, November 2005.

[36] U. Mettin, *Principles for Planning and Analyzing Motions of Underactuated Mechanical Systems and Redundant Manipulators*. PhD thesis, Umea University, 2009.

[37] U. Mettin, A. S. Shiriaev, L. B. Freidovich, and M. Sampei, "Optimal ball pitching with an actuated model of a human arm," in *IEEE International Conference on Robotics and Automation*, 2010.

[38] B. Vanderborght, N. Tsagarakis, R. Ham, I. Thorson, and D. Caldwell, "Maccepa 2.0: compliant actuator used for energy efficient hopping robot chobino1d," *Autonomous Robots*, vol. 31, pp. 55–65, 2011.

[39] H. Frank, "Design and simulation of a numerical controlled throwing device," in *Modeling Simulation, 2008. AICMS 08. Second Asia International Conference on*, pp. 777 –782, may 2008.

[40] H. Frank, A. Mittnacht, T. Moschinsky, and F. Kupzog, "1-dof-robot for fast and accurate throwing of objects," in *Emerging Technologies Factory Automation, 2009. ETFA 2009. IEEE Conference on*, pp. 1 –7, sept. 2009.

[41] H. Geyer, *Simple Models of Legged Locomotion based on Compliant Limb Behavior*. PhD thesis, der Friedrich-Schiller-Universitat Jena, 2005.

[42] J. W. Hurst, J. E. Chestnutt, and A. A. Rizzi, "Series compliance for an efficient running gait: Lessons learned from the ecd leg," *IEEE Robotics and Automation Magazine*, vol. September, pp. 42–51, 2008.

[43] J. Hurst, J. Chestnutt, and A. Rizzi, "The actuator with mechanically adjustable series compliance," *Robotics, IEEE Transactions on*, vol. 26, pp. 597 –606, aug. 2010.

[44] J. D. Schutter, "A study of active compliant motion control methods for rigid manipulators based on a generic control scheme," in *IEEE International Conference on Robotics and Automation*, pp. 1060–1065, 1987.

[45] G. A. Pratt and M. M. Williamson, "Series elastic actuators," in *IEEE International Conference on Intelligent Robots and Systems*, vol. 1, pp. 399–406, 1995.

[46] J. W. Hurst, D. Hobbelen, and A. A. Rizzi, "Series elastic actuation: Potential and pitfalls," in *IROS Workshop*, 2005.

[47] S. Haddadin, N. Mansfeld, and A. Albu-Schaffer, "Rigid vs. elastic actuation: Requirements and performance," in *Intelligent Robots and Systems (IROS), 2012 IEEE/RSJ International Conference on*, pp. 5097 –5104, oct. 2012.

[48] D. Braun, M. Howard, and S. Vijayakumar, "Optimal variable stiffness control: formulation and application to explosive movement tasks," *Autonomous Robots*, vol. 33, pp. 237–253, 2012.

[49] M. Garabini, A. Passaglia, F. Belo, P. Salaris, and A. Bicchi, "Optimality principles in stiffness control: The vsa kick," in *Robotics and Automation (ICRA), 2012 IEEE International Conference on*, pp. 3341 –3346, may 2012.

[50] R. Clough and J. Penzien, *Dynamics of Structures*. McGraw-Hill, 2002.